

Easy axis crystal field limit in trivalent lanthanide complexes: expected magnetization, susceptibility, magnetic torque and XMCD signatures.

Leonardo Tacconi^{†*} and Mauro Perfetti^{†*}

[†] Department of Chemistry “Ugo Schiff” & INSTM RU, Università degli Studi di Firenze, Via della Lastruccia 3, 50019, Sesto F.no (FI), Italy

*leonardo.tacconi@unifi.it, *mauro.perfetti@unifi.it

Supporting Information

Table of Contents

Supporting Figures	5
Figure S1 – Asphericity of the J, mJ components of Ln(III) ions, calculated using equations reported by Sievers.....	5
Figure S2 – Magnetization curves of an ideal axial Dy(III) ion simulated at 2K for a powder ensemble with different energy separations ΔE between the ground and first excited doublets.....	5
Figure S3 – Field dependence of the magnetization of an ideal axial Dy(III) ion simulated at 2K for a powder ensemble (black), and with the magnetic field applied along the z axis (blue) and the xy plane (red).	6
Figure S4 – Expected magnetization values calculated for lanthanide ions with an easy-axis magnetic anisotropy and comparison with the magnetization values calculated using the thirds approximation.	6
Figure S5 – Comparison between the simulated values of powder magnetization for an easy-axis Dy(III) centre using a proper sphere sampling (lines) and the thirds averaging (dashed lines) in the low-temperature regime.....	7
Figure S6 – Simulated powder and single-crystal magnetization values for a Dy ³⁺ ion with a ground state doublet composed of 4% $13/2$ + 21% $11/2$ + 40% $9/2$ + 22% $7/2$ + 7% $5/2$..	7
Figure S7 – Expected χT values calculated for lanthanide ions with an easy-axis magnetic anisotropy and comparison with the χT values calculated using the thirds approximation. .	8
Figure S8 – Cantilever torque magnetometry curves simulated at T = 2 K for a Ce(III) centre having a negative value for B_{20} , as discussed in main text.	8

Figure S9 – Cantilever torque magnetometry curves simulated at $T = 2$ K for a Pr(III) centre having a negative value for B_{20} , as discussed in main text.	9
Figure S10 – Cantilever torque magnetometry curves simulated at $T = 2$ K for a Nd(III) centre having a negative value for B_{20} , as discussed in main text.	9
Figure S11 – Cantilever torque magnetometry curves simulated at $T = 2$ K for a Pm(III) centre having a negative value for B_{20} , as discussed in main text.	10
Figure S12 – Cantilever torque magnetometry curves simulated at $T = 2$ K for a Sm(III) centre having a negative value for B_{20} , as discussed in main text.	10
Figure S13 – Cantilever torque magnetometry curves simulated at $T = 2$ K for a Tb(III) centre having a negative value for B_{20} , as discussed in main text.	11
Figure S14 – Cantilever torque magnetometry curves simulated at $T = 2$ K for a Dy(III) centre having a negative value for B_{20} , as discussed in main text.	11
Figure S15 – Cantilever torque magnetometry curves simulated at $T = 2$ K for a Ho(III) centre having a negative value for B_{20} , as discussed in main text.	12
Figure S16 – Cantilever torque magnetometry curves simulated at $T = 2$ K for a Er(III) centre having a negative value for B_{20} , as discussed in main text.	12
Figure S17 – Cantilever torque magnetometry curves simulated at $T = 2$ K for a Tm(III) centre having a negative value for B_{20} , as discussed in main text.	13
Figure S18 – Cantilever torque magnetometry curves simulated at $T = 2$ K for a Yb(III) centre having a negative value for B_{20} , as discussed in main text.	13
Figure S19 – Angular dependent XMCD spectra at 6 T (a) and angular- and field-dependent XMCD maximum values at M_5 (b) and M_4 (c) edges for Ce(III) centre having a negative B_{20} value, as discussed in main text.	14
Figure S20 – Angular dependent XMCD spectra at 6 T (a) and angular- and field-dependent XMCD maximum values at M_5 (b) and M_4 (c) edges for Pr(III) centre having a negative B_{20} value, as discussed in main text.	15
Figure S21 – Angular dependent XMCD spectra at 6 T (a) and angular- and field-dependent XMCD maximum values at M_5 (b) and M_4 (c) edges for Nd(III) centre having a negative B_{20} value, as discussed in main text.	16
Figure S22 – Angular dependent XMCD spectra at 6 T (a) and angular- and field-dependent XMCD maximum values at M_5 (b) and M_4 (c) edges for Pm(III) centre having a negative B_{20} value, as discussed in main text.	17
Figure S23 – Angular dependent XMCD spectra at 6 T (a) and angular- and field-dependent XMCD maximum values at M_5 (b) and M_4 (c) edges for Sm(III) centre having a negative B_{20} value, as discussed in main text.	18

Figure S24 – Angular dependent XMCD spectra at 6 T (a) and angular- and field-dependent XMCD maximum values at M ₅ (b) and M ₄ (c) edges for Tb(III) centre having a negative <i>B</i> 20 value, as discussed in main text.	19
Figure S25 – Angular dependent XMCD spectra at 6 T (a) and angular- and field-dependent XMCD maximum values at M ₅ (b) and M ₄ (c) edges for Dy(III) centre having a negative <i>B</i> 20 value, as discussed in main text.	20
Figure S26 – Angular dependent XMCD spectra at 6 T (a) and angular- and field-dependent XMCD maximum values at M ₅ (b) and M ₄ (c) edges for Ho(III) centre having a negative <i>B</i> 20 value, as discussed in main text.	21
Figure S27 – Angular dependent XMCD spectra at 6 T (a) and angular- and field-dependent XMCD maximum values at M ₅ (b) and M ₄ (c) edges for Er(III) centre having a negative <i>B</i> 20 value, as discussed in main text.	22
Figure S28 – Angular dependent XMCD spectra at 6 T (a) and angular- and field-dependent XMCD maximum values at M ₅ (b) and M ₄ (c) edges for Tm(III) centre having a negative <i>B</i> 20 value, as discussed in main text.	23
Figure S29 – Angular dependent XMCD spectra at 6 T (a) and angular- and field-dependent XMCD maximum values at M ₅ (b) edge for Yb(III) centre having a negative <i>B</i> 20 value, as discussed in main text.	24
Supporting Tables	25
Table S1 – <i>B</i> 20 values used for simulating all the magnetic observables of all lanthanide tripositive ions and the associated energy structure of the ground state J multiplet.	25
Table S2 – Angular- and field-dependent XMCD maximum values at M _{4,5} edges for Ce(III) centre having a negative <i>B</i> 20 value, as discussed in main text.	26
Table S3 – Angular- and field-dependent XMCD maximum values at M _{4,5} edges for Pr(III) centre having a negative <i>B</i> 20 value, as discussed in main text.	27
Table S4 – Angular- and field-dependent XMCD maximum values at M _{4,5} edges for Nd(III) centre having a negative <i>B</i> 20 value, as discussed in main text.	28
Table S5 – Angular- and field-dependent XMCD maximum values at M _{4,5} edges for Pm(III) centre having a negative <i>B</i> 20 value, as discussed in main text.	29
Table S6 – Angular- and field-dependent XMCD maximum values at M _{4,5} edges for Sm(III) centre having a negative <i>B</i> 20 value, as discussed in main text.	30
Table S7 – Angular- and field-dependent XMCD maximum values at M _{4,5} edges for Tb(III) centre having a negative <i>B</i> 20 value, as discussed in main text.	31
Table S8 – Angular- and field-dependent XMCD maximum values at M _{4,5} edges for Dy(III) centre having a negative <i>B</i> 20 value, as discussed in main text.	32
Table S9 – Angular- and field-dependent XMCD maximum values at M _{4,5} edges for Ho(III) centre having a negative <i>B</i> 20 value, as discussed in main text.	33

Table S10 – Angular- and field-dependent XMCD maximum values at $M_{4,5}$ edges for Er(III) centre having a negative B_{20} value, as discussed in main text.	34
Table S11 – Angular- and field-dependent XMCD maximum values at $M_{4,5}$ edges for Tm(III) centre having a negative B_{20} value, as discussed in main text.	35
Table S12 – Angular- and field-dependent XMCD maximum values at $M_{4,5}$ edges for Yb(III) centre having a negative B_{20} value, as discussed in main text.	36
Supporting Notes	37
Note S1. Normalization procedure of XMCD spectra.	37

Supporting Figures

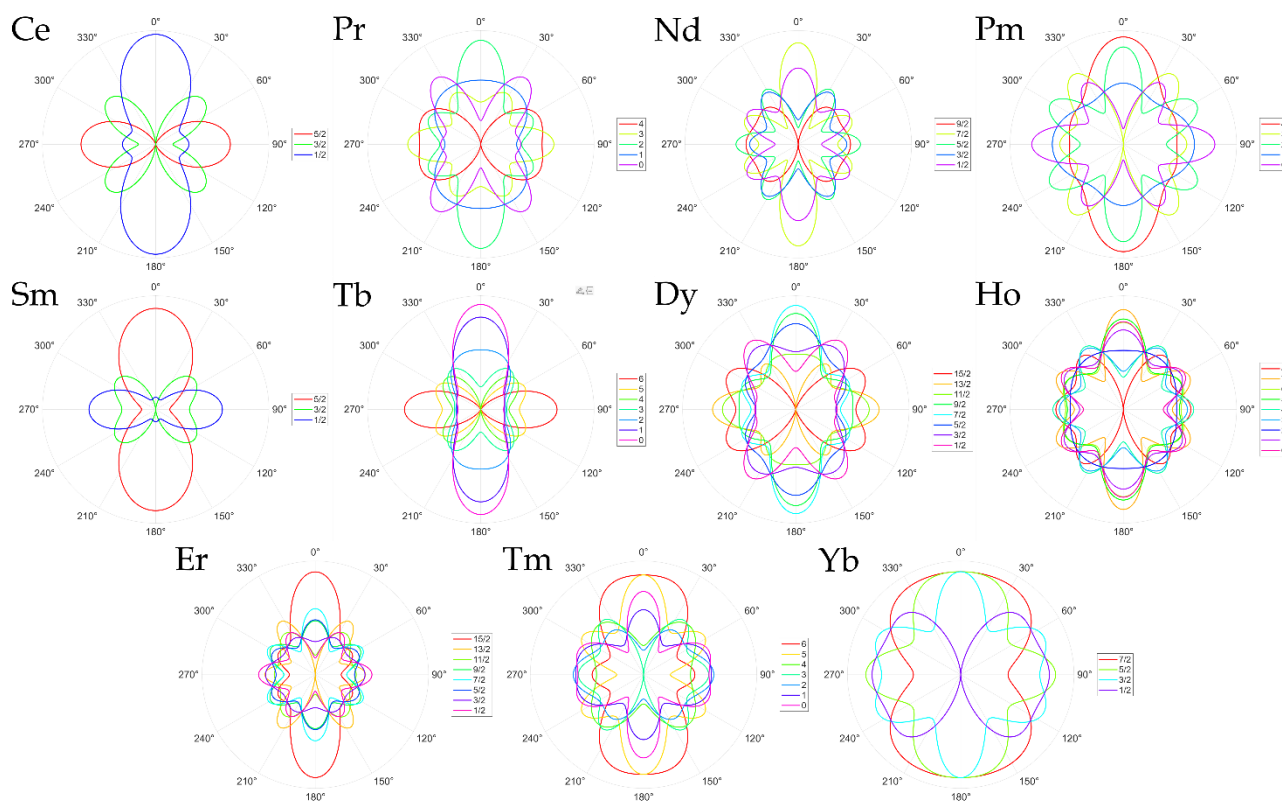


Figure S1 – Asphericity of the $|J, m_J\rangle$ components of Ln(III) ions, calculated using equations reported by Sievers.

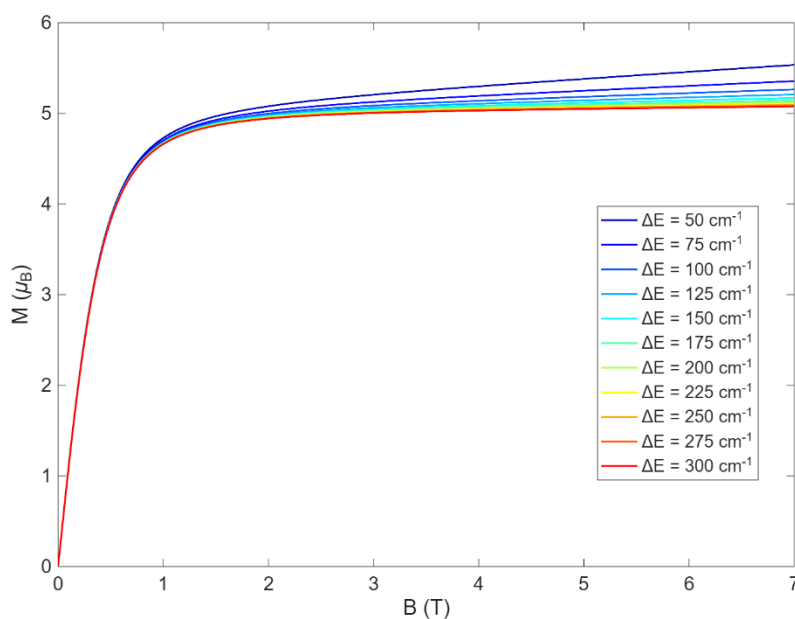


Figure S2 – Magnetization curves of an ideal axial Dy(III) ion simulated at 2K for a powder ensemble with different energy separations ΔE between the ground and first excited doublets.

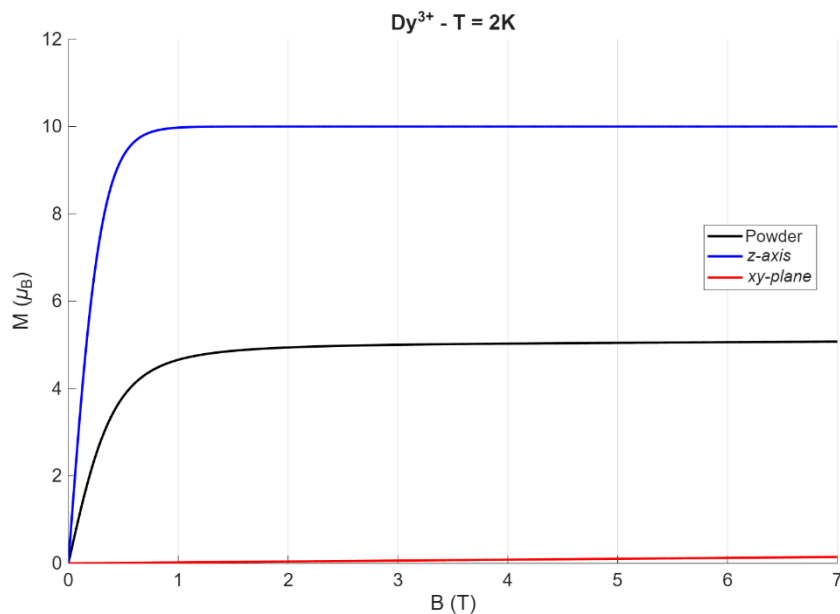


Figure S3 – Field dependence of the magnetization of an ideal axial Dy(III) ion simulated at 2K for a powder ensemble (black), and with the magnetic field applied along the z axis (blue) and the xy plane (red).

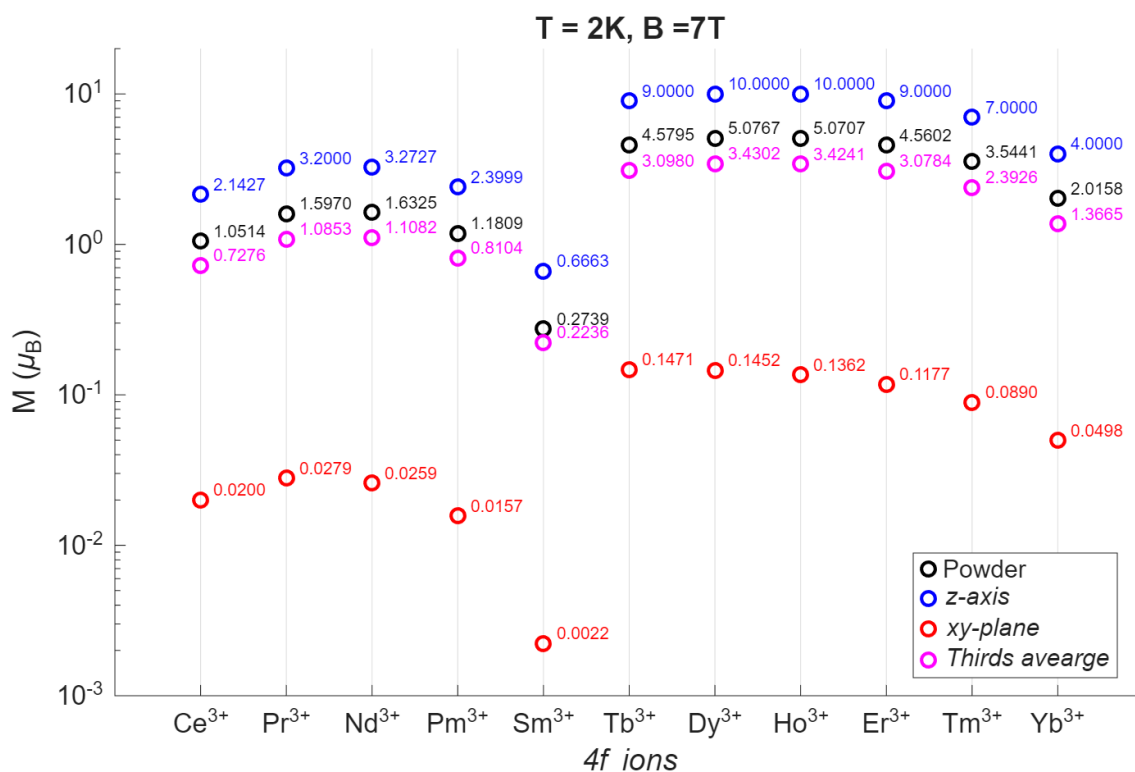


Figure S4 – Expected magnetization values calculated for lanthanide ions with an easy-axis magnetic anisotropy and comparison with the magnetization values calculated using the thirds approximation.

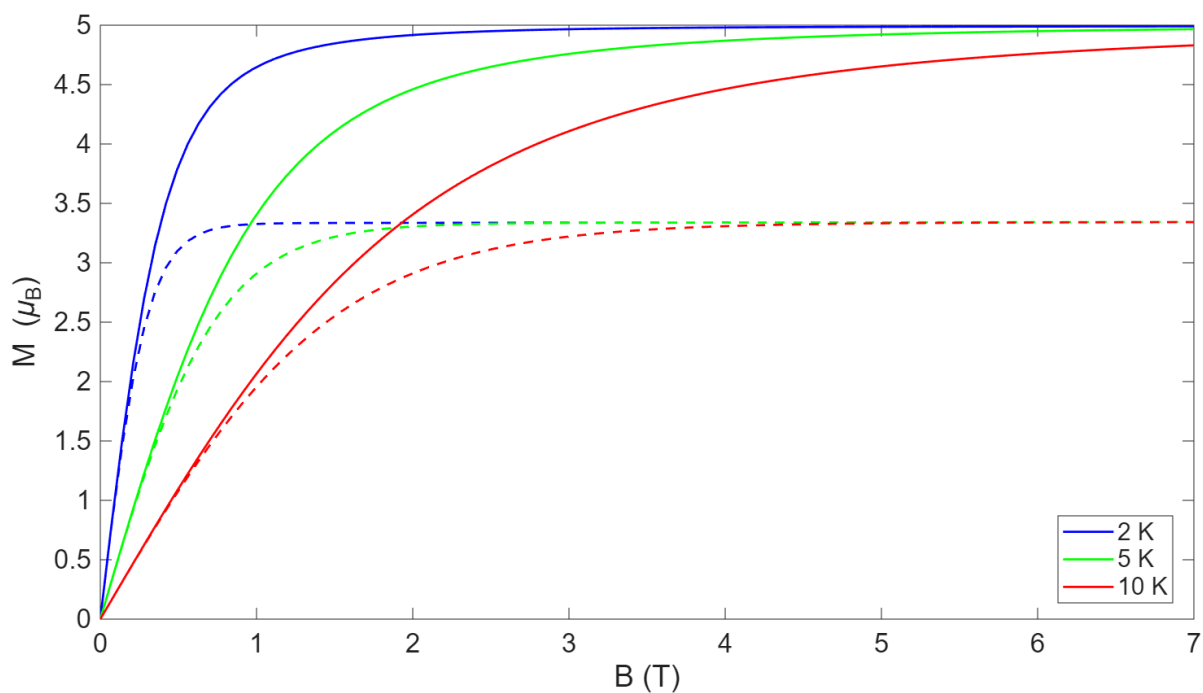


Figure S5 – Comparison between the simulated values of powder magnetization for an easy-axis Dy(III) centre using a proper sphere sampling (lines) and the third-order averaging (dashed lines) in the low-temperature regime.

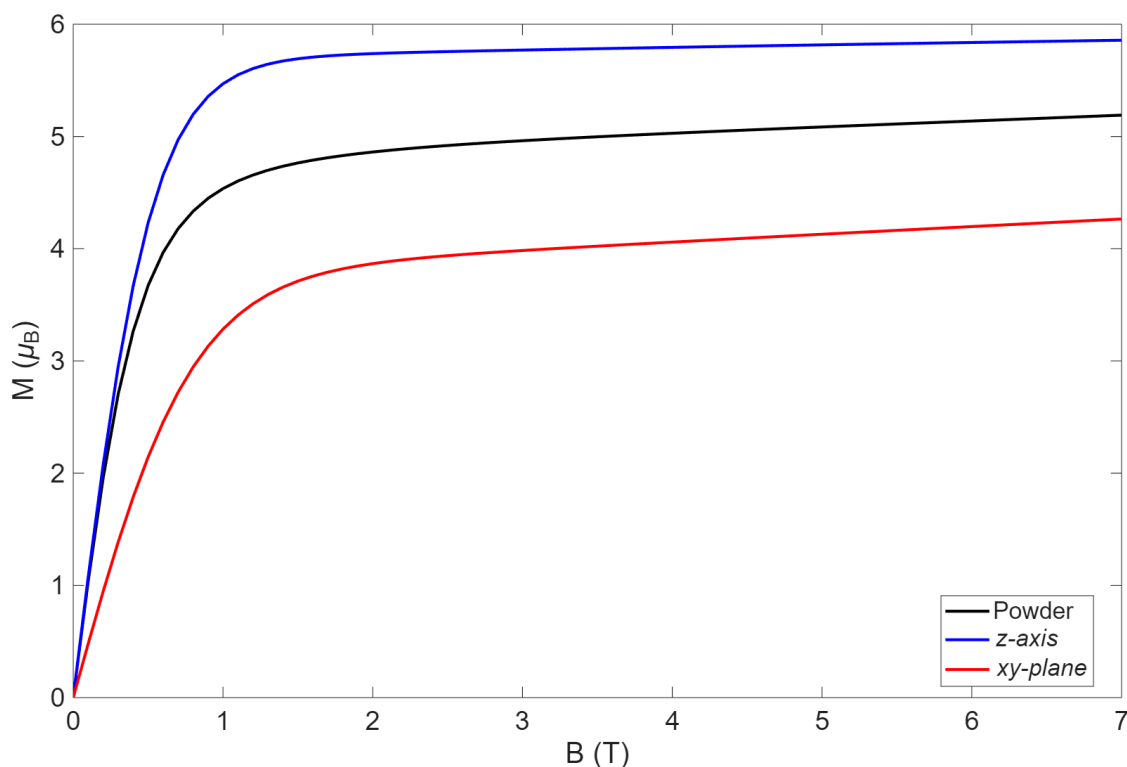


Figure S6 – Simulated powder and single-crystal magnetization values for a Dy^{3+} ion with a ground state doublet composed of $4\%|13/2\rangle + 21\%|11/2\rangle + 40\%|9/2\rangle + 22\%|7/2\rangle + 7\%|5/2\rangle$.

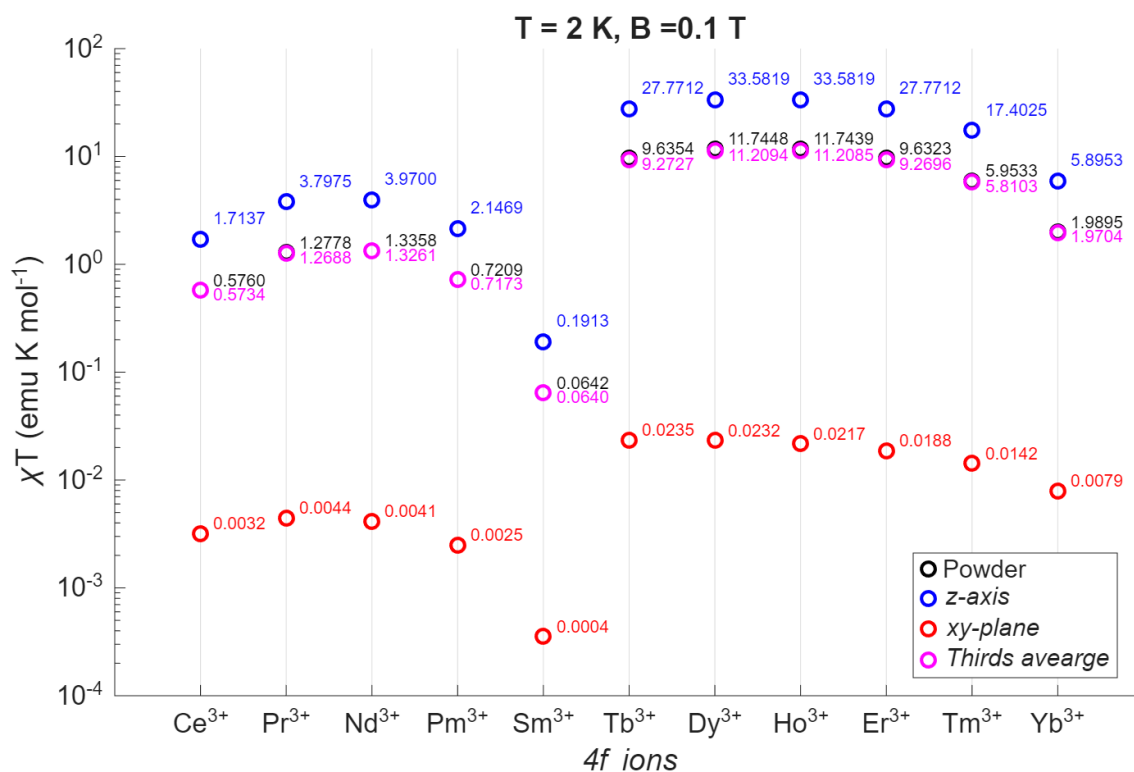


Figure S7 – Expected χT values calculated for lanthanide ions with an easy-axis magnetic anisotropy and comparison with the χT values calculated using the thirds approximation.

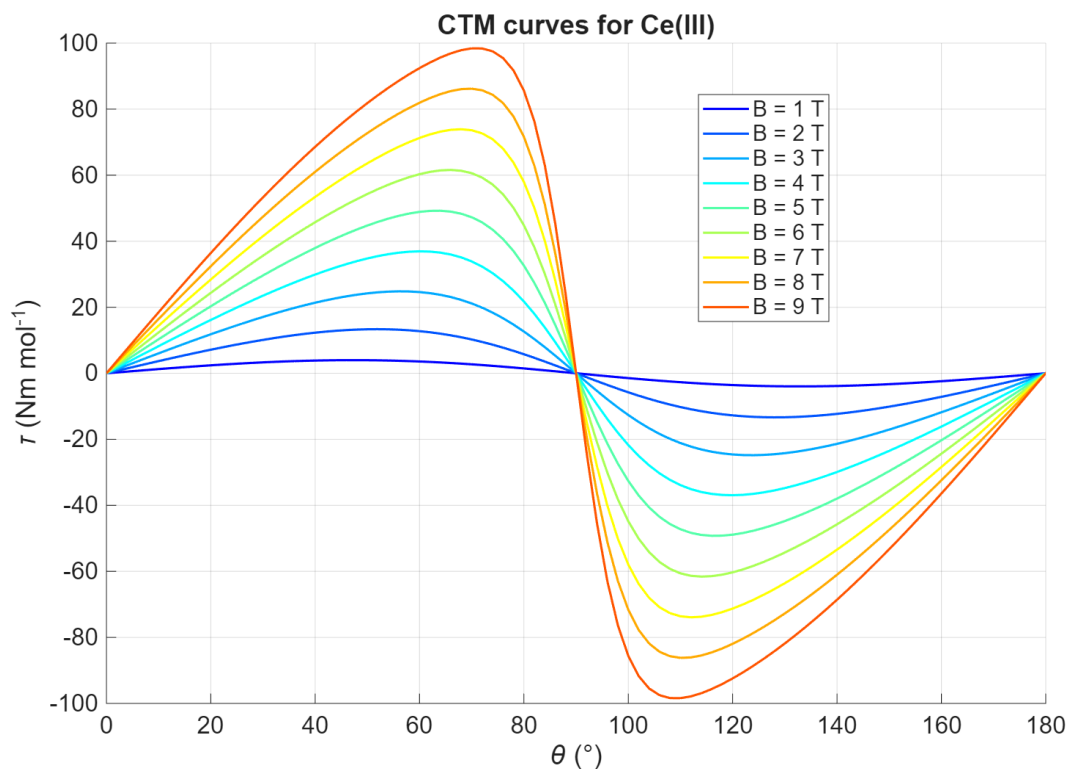


Figure S8 – Cantilever torque magnetometry curves simulated at T = 2 K for a Ce(III) centre having a negative value for B_2^0 , as discussed in main text.

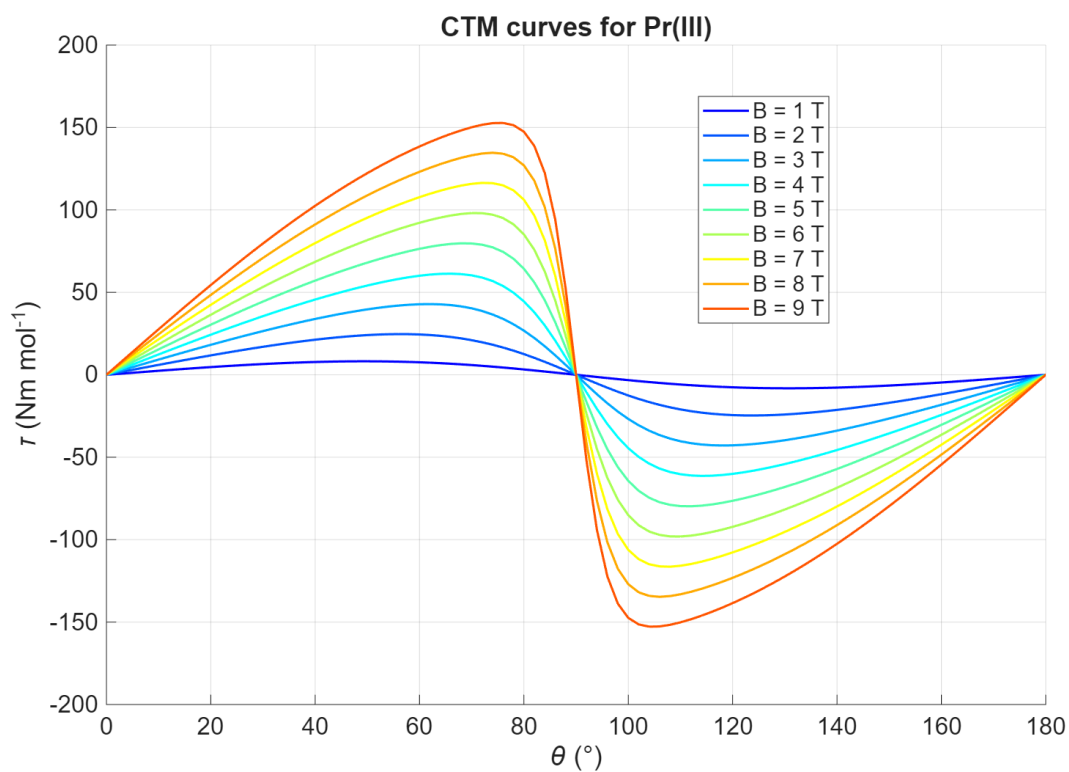


Figure S9 – Cantilever torque magnetometry curves simulated at $T = 2$ K for a Pr(III) centre having a negative value for B_2^0 , as discussed in main text.

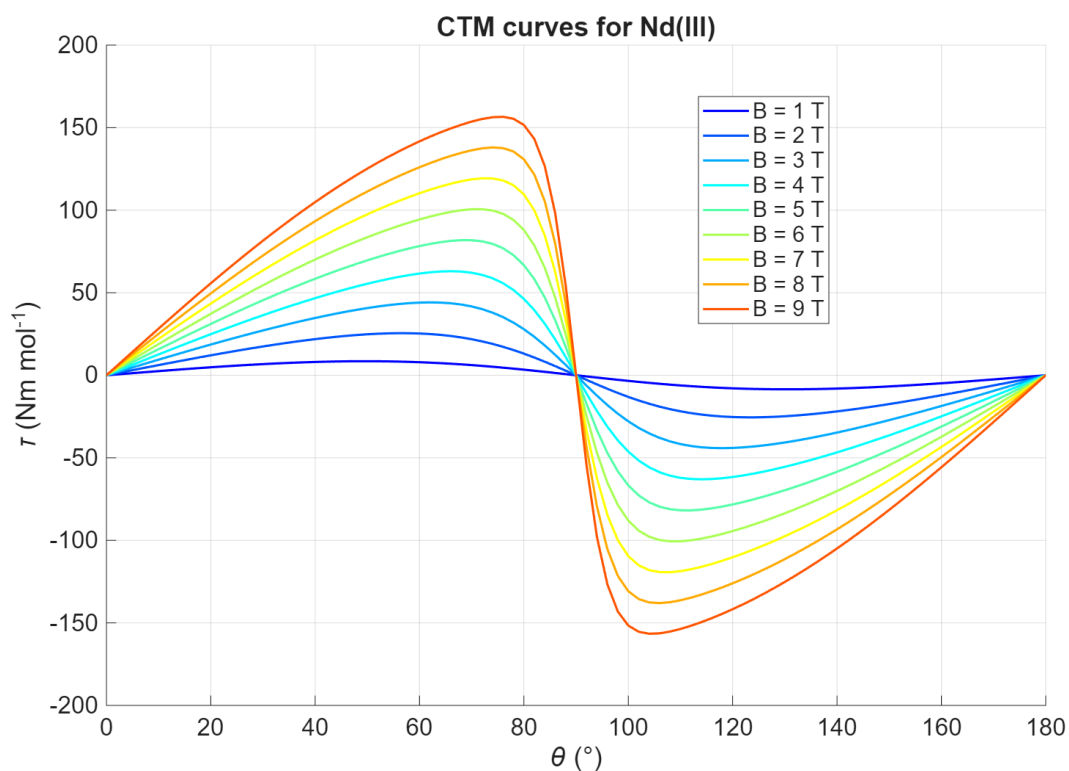


Figure S10 – Cantilever torque magnetometry curves simulated at $T = 2$ K for a Nd(III) centre having a negative value for B_2^0 , as discussed in main text.

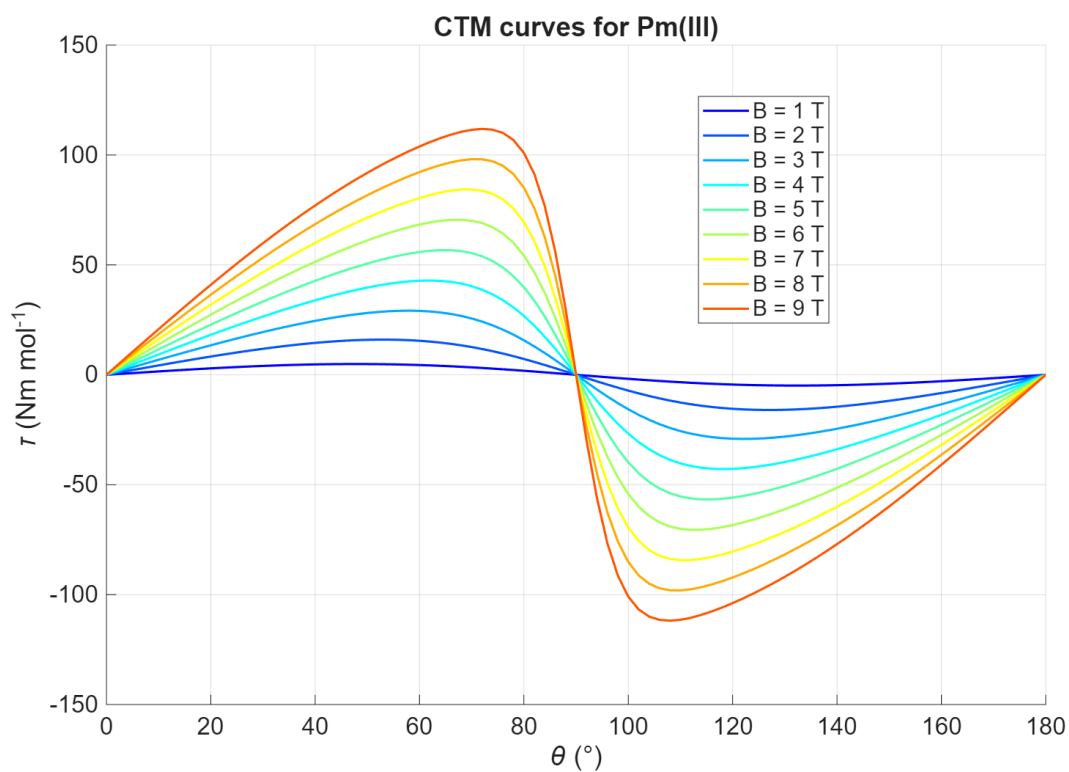


Figure S11 – Cantilever torque magnetometry curves simulated at $T = 2$ K for a Pm(III) centre having a negative value for B_2^0 , as discussed in main text.

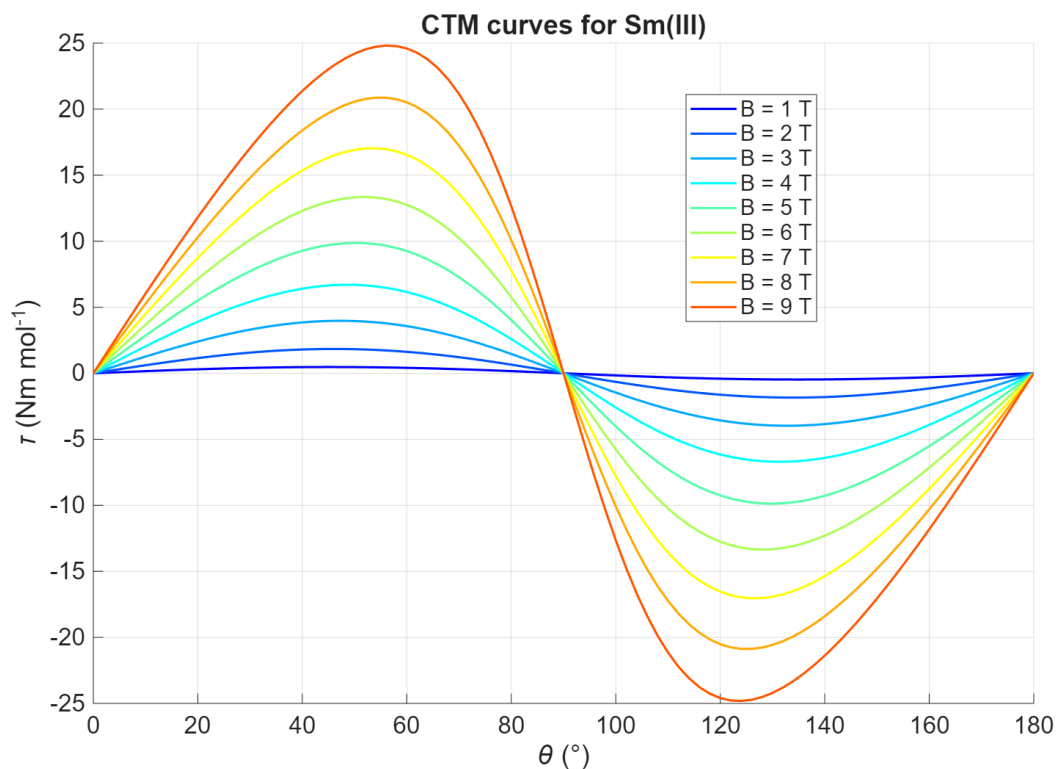


Figure S12 – Cantilever torque magnetometry curves simulated at $T = 2$ K for a Sm(III) centre having a negative value for B_2^0 , as discussed in main text.

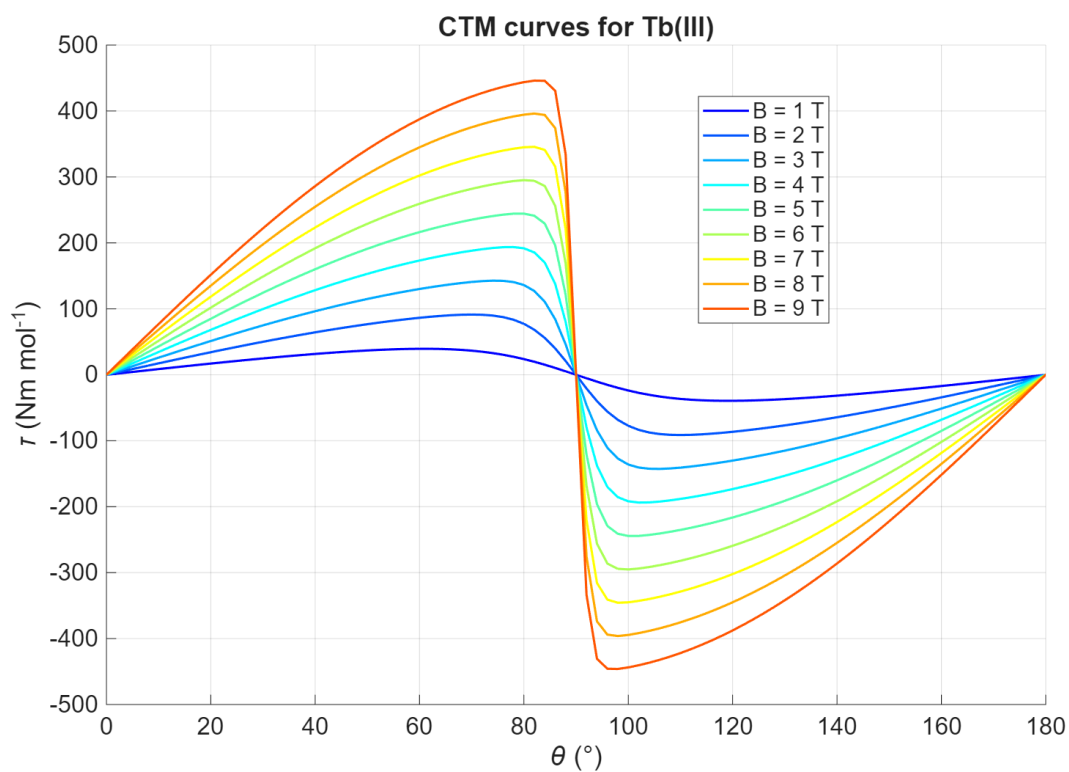


Figure S13 – Cantilever torque magnetometry curves simulated at T = 2 K for a Tb(III) centre having a negative value for B_2^0 , as discussed in main text.

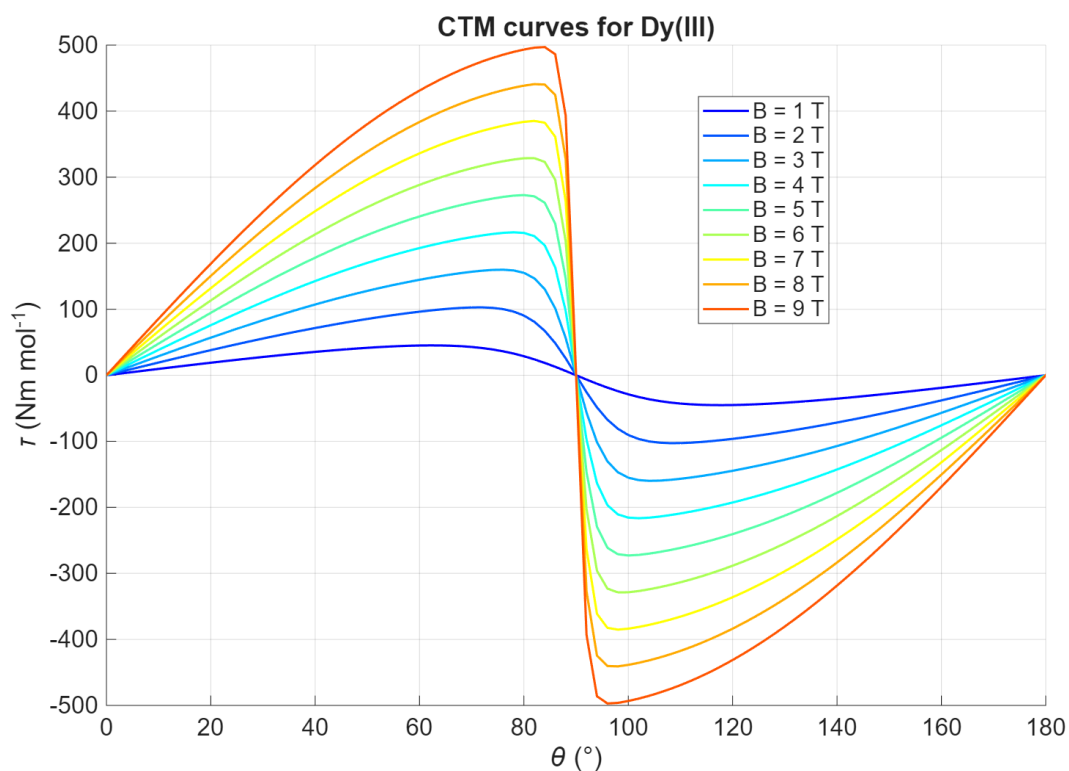


Figure S14 – Cantilever torque magnetometry curves simulated at T = 2 K for a Dy(III) centre having a negative value for B_2^0 , as discussed in main text.

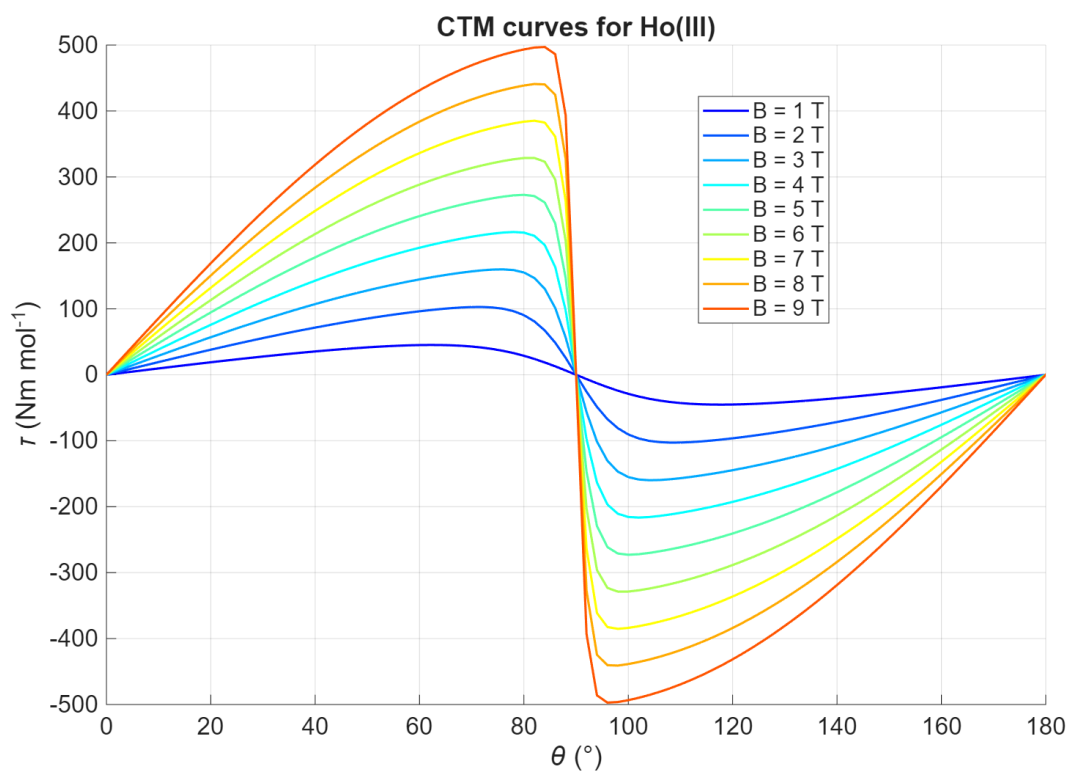


Figure S15 – Cantilever torque magnetometry curves simulated at $T = 2 \text{ K}$ for a Ho(III) centre having a negative value for B_2^0 , as discussed in main text.

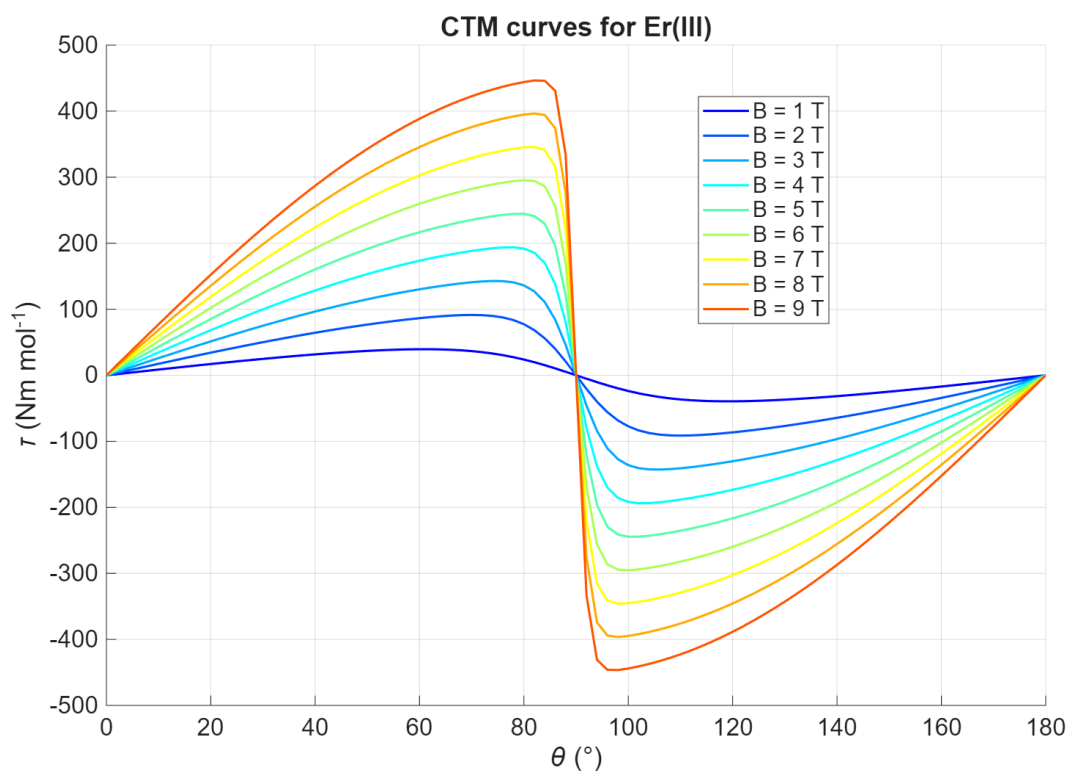


Figure S16 – Cantilever torque magnetometry curves simulated at $T = 2 \text{ K}$ for a Er(III) centre having a negative value for B_2^0 , as discussed in main text.

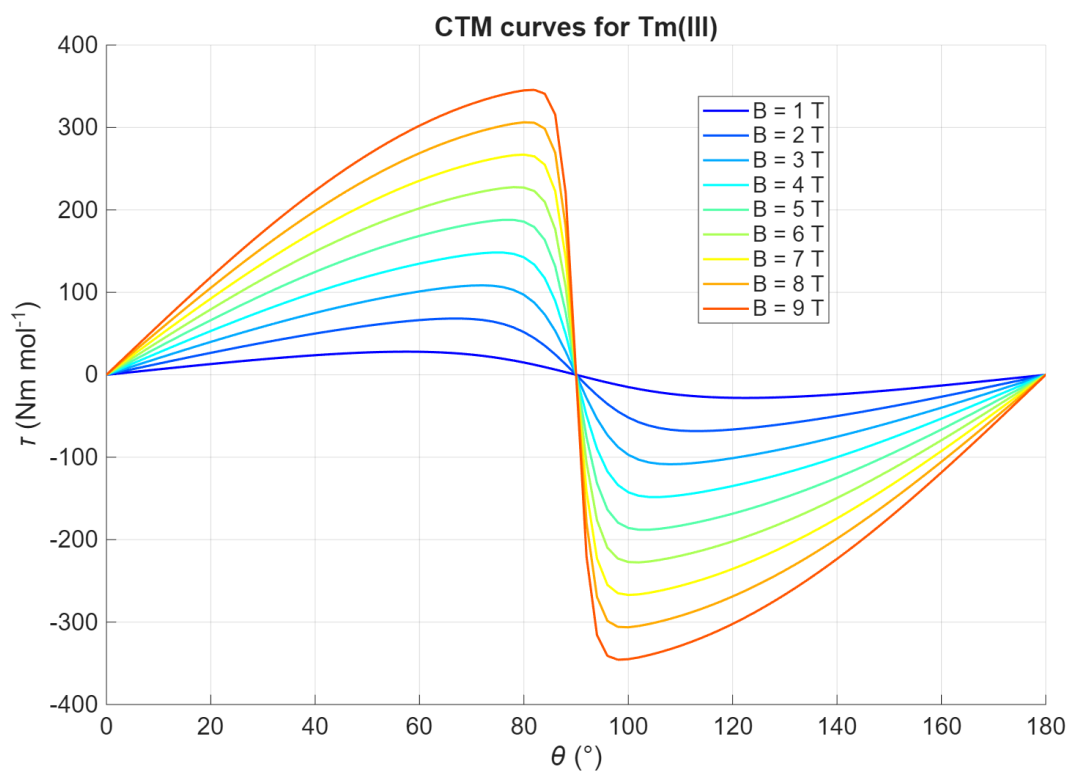


Figure S17 – Cantilever torque magnetometry curves simulated at $T = 2$ K for a Tm(III) centre having a negative value for B_2^0 , as discussed in main text.

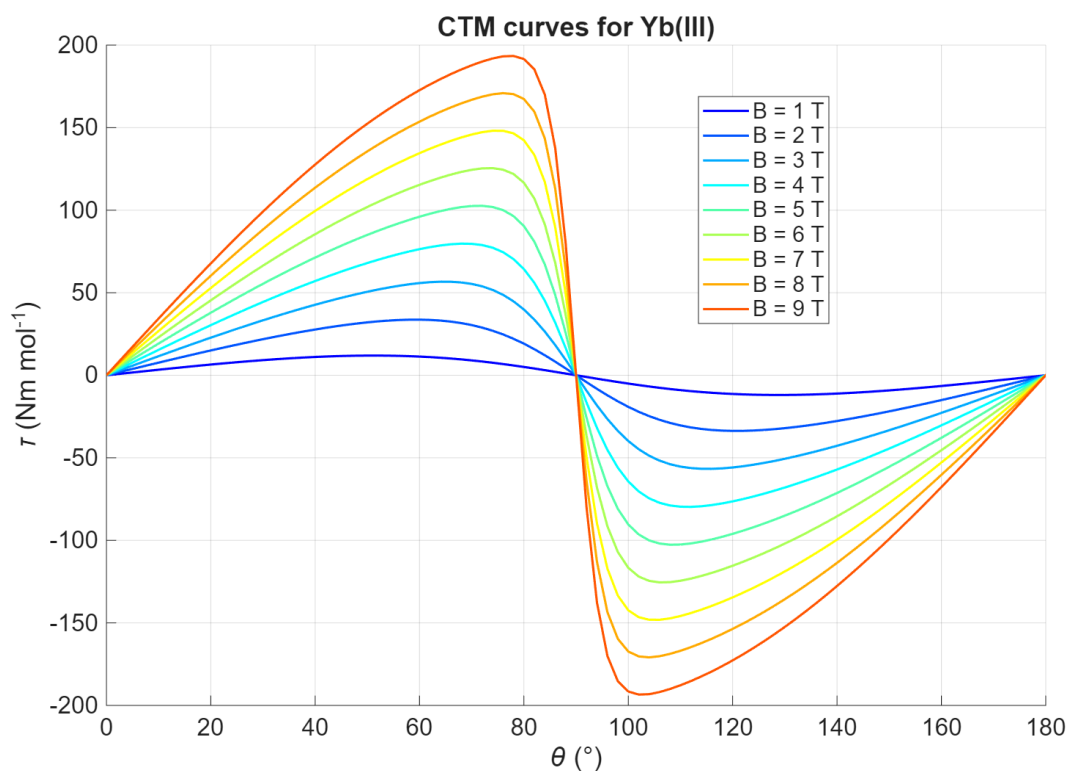


Figure S18 – Cantilever torque magnetometry curves simulated at $T = 2$ K for a Yb(III) centre having a negative value for B_2^0 , as discussed in main text.

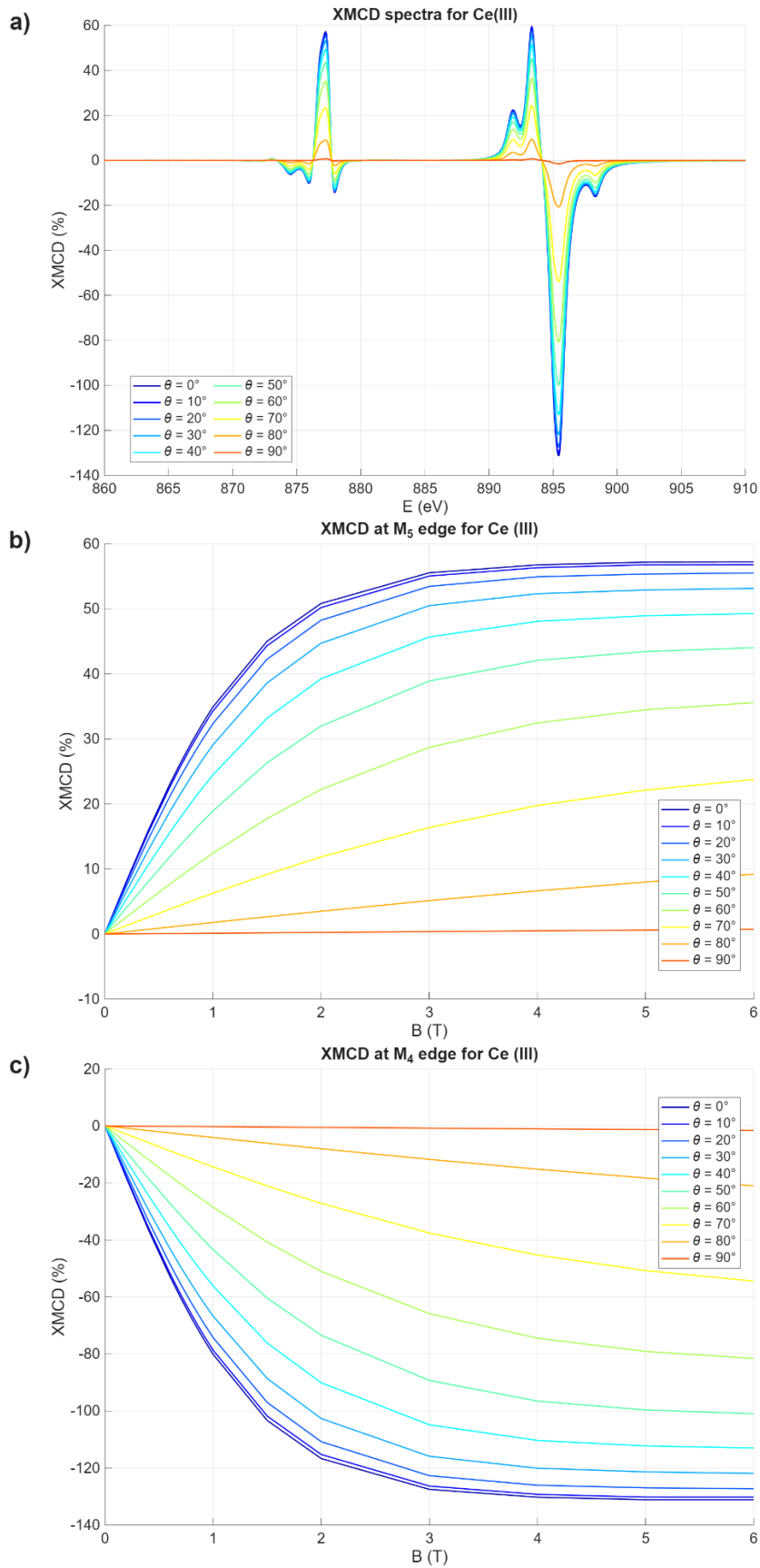


Figure S19 – Angular dependent XMCD spectra at 6 T (a) and angular- and field-dependent XMCD maximum values at M_5 (b) and M_4 (c) edges for Ce(III) centre having a negative B_2^0 value, as discussed in main text.

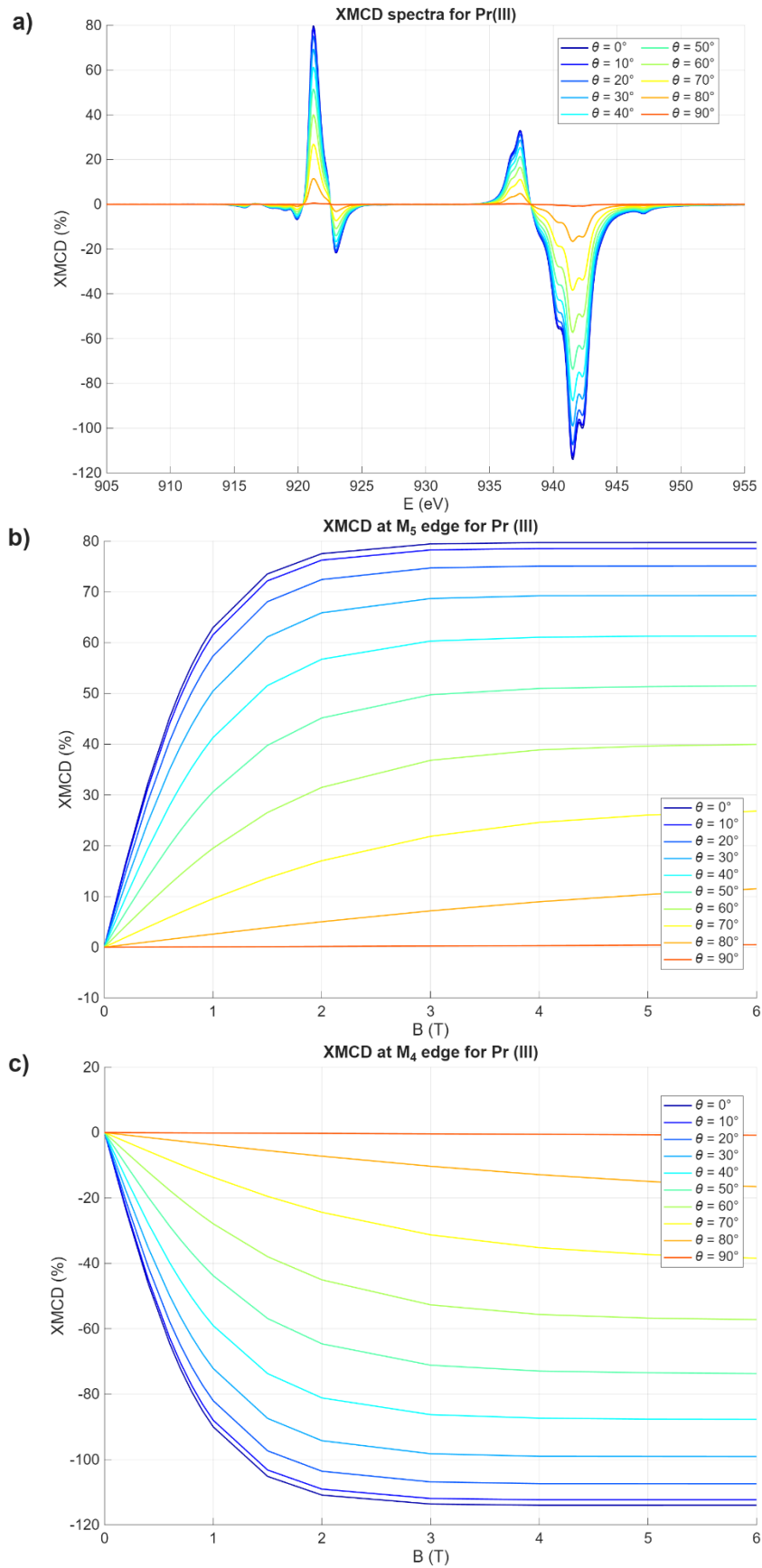


Figure S20 – Angular dependent XMCD spectra at 6 T (a) and angular- and field-dependent XMCD maximum values at M_5 (b) and M_4 (c) edges for Pr(III) centre having a negative B_2^0 value, as discussed in main text.

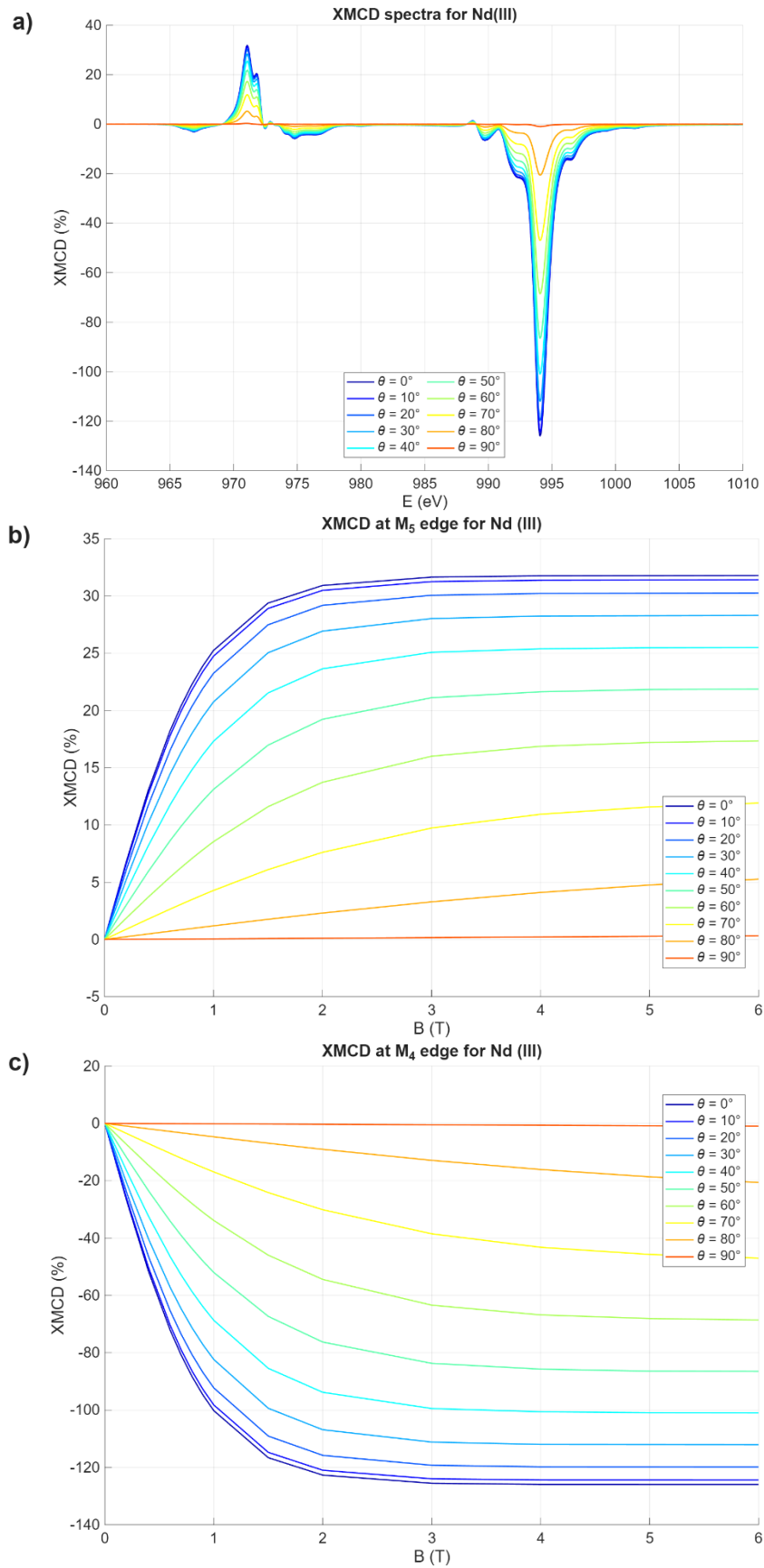


Figure S21 – Angular dependent XMCD spectra at 6 T (a) and angular- and field-dependent XMCD maximum values at M_5 (b) and M_4 (c) edges for Nd(III) centre having a negative B_2^0 value, as discussed in main text.

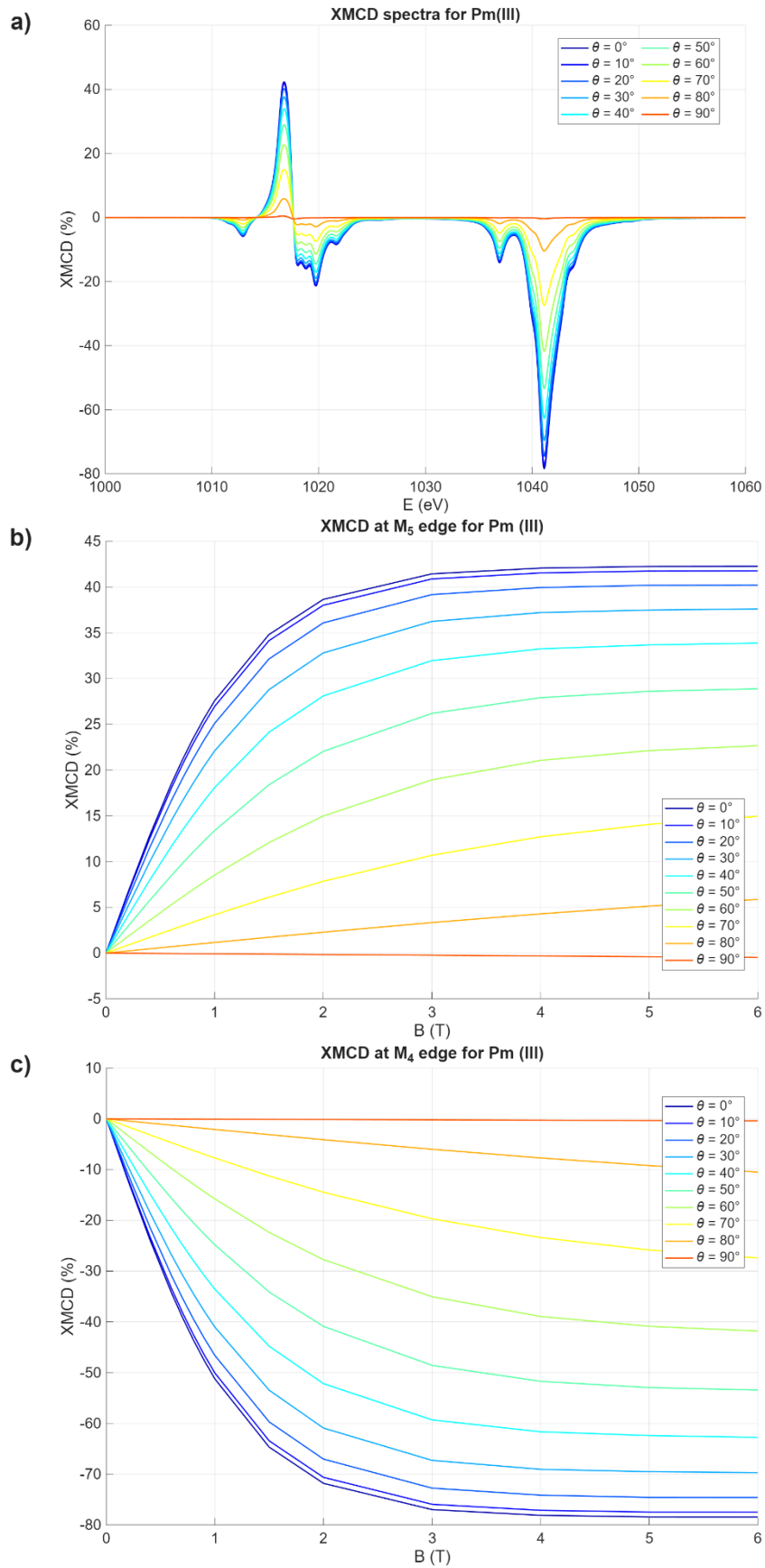


Figure S22 – Angular dependent XMCD spectra at 6 T (a) and angular- and field-dependent XMCD maximum values at M_5 (b) and M_4 (c) edges for Pm(III) centre having a negative B_2^0 value, as discussed in main text.

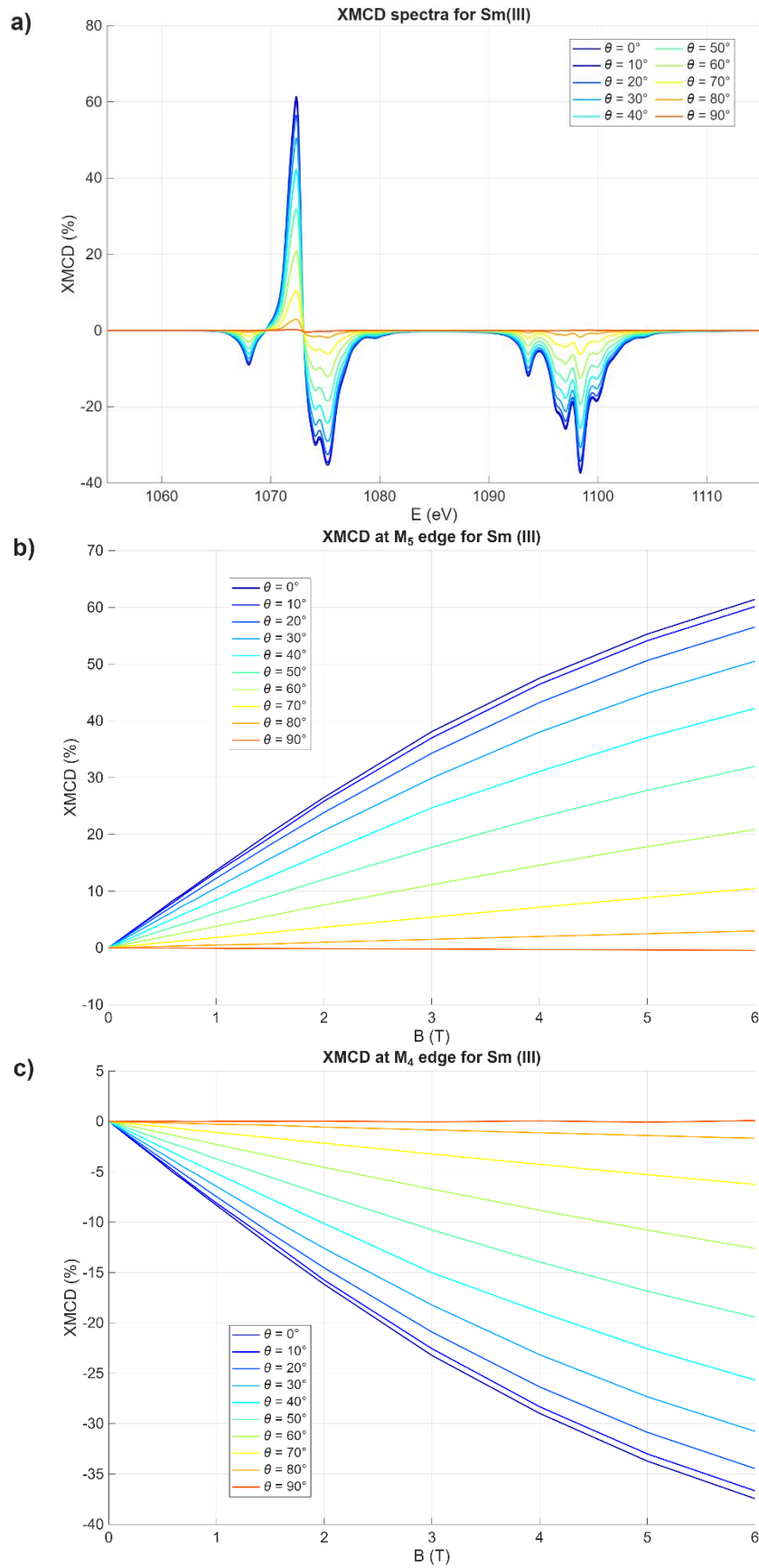


Figure S23 – Angular dependent XMCD spectra at 6 T (a) and angular- and field-dependent XMCD maximum values at M_5 (b) and M_4 (c) edges for Sm(III) centre having a negative B_2^0 value, as discussed in main text.

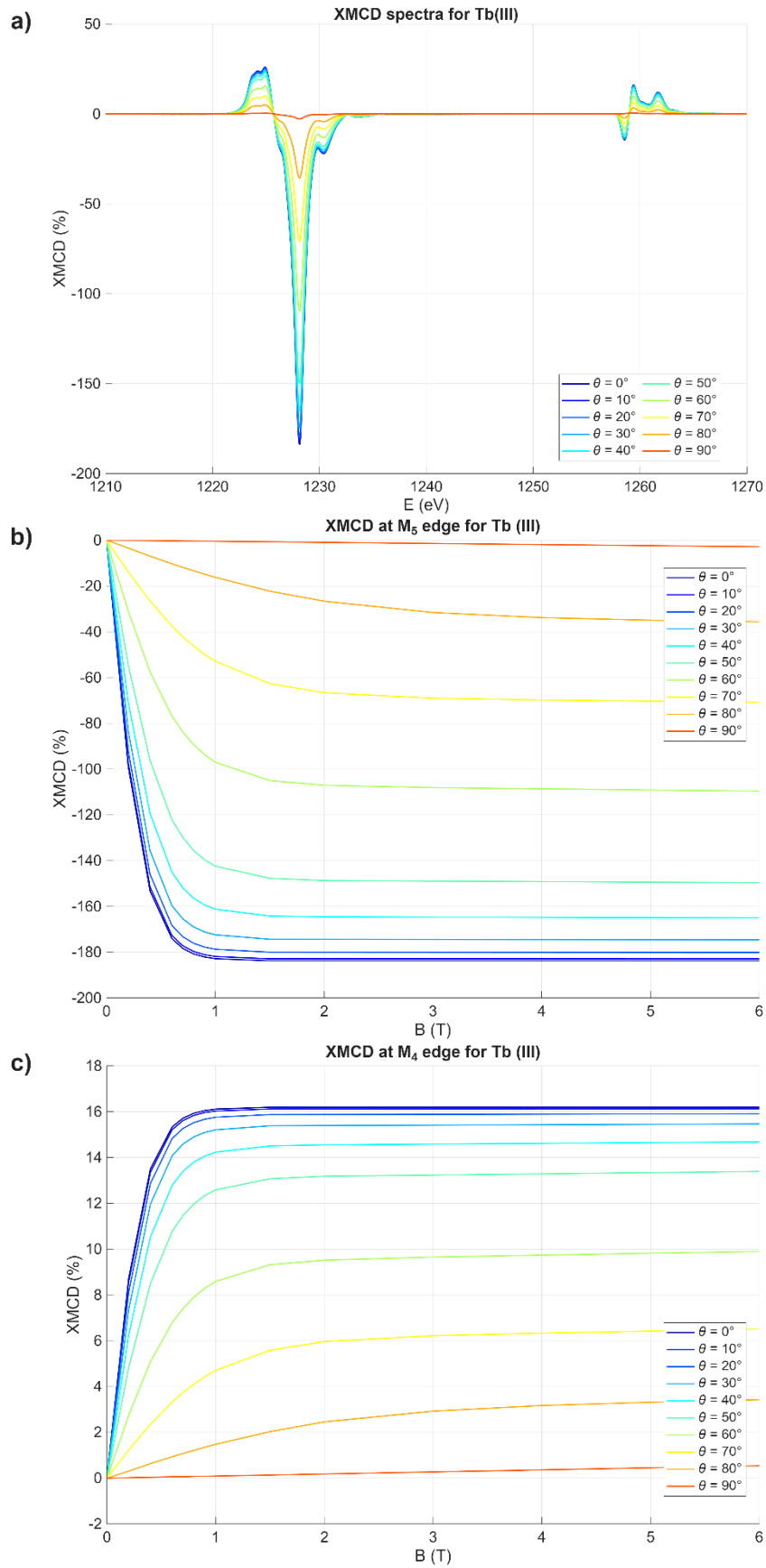


Figure S24 – Angular dependent XMCD spectra at 6 T (a) and angular- and field-dependent XMCD maximum values at M_5 (b) and M_4 (c) edges for Tb(III) centre having a negative B_2^0 value, as discussed in main text.

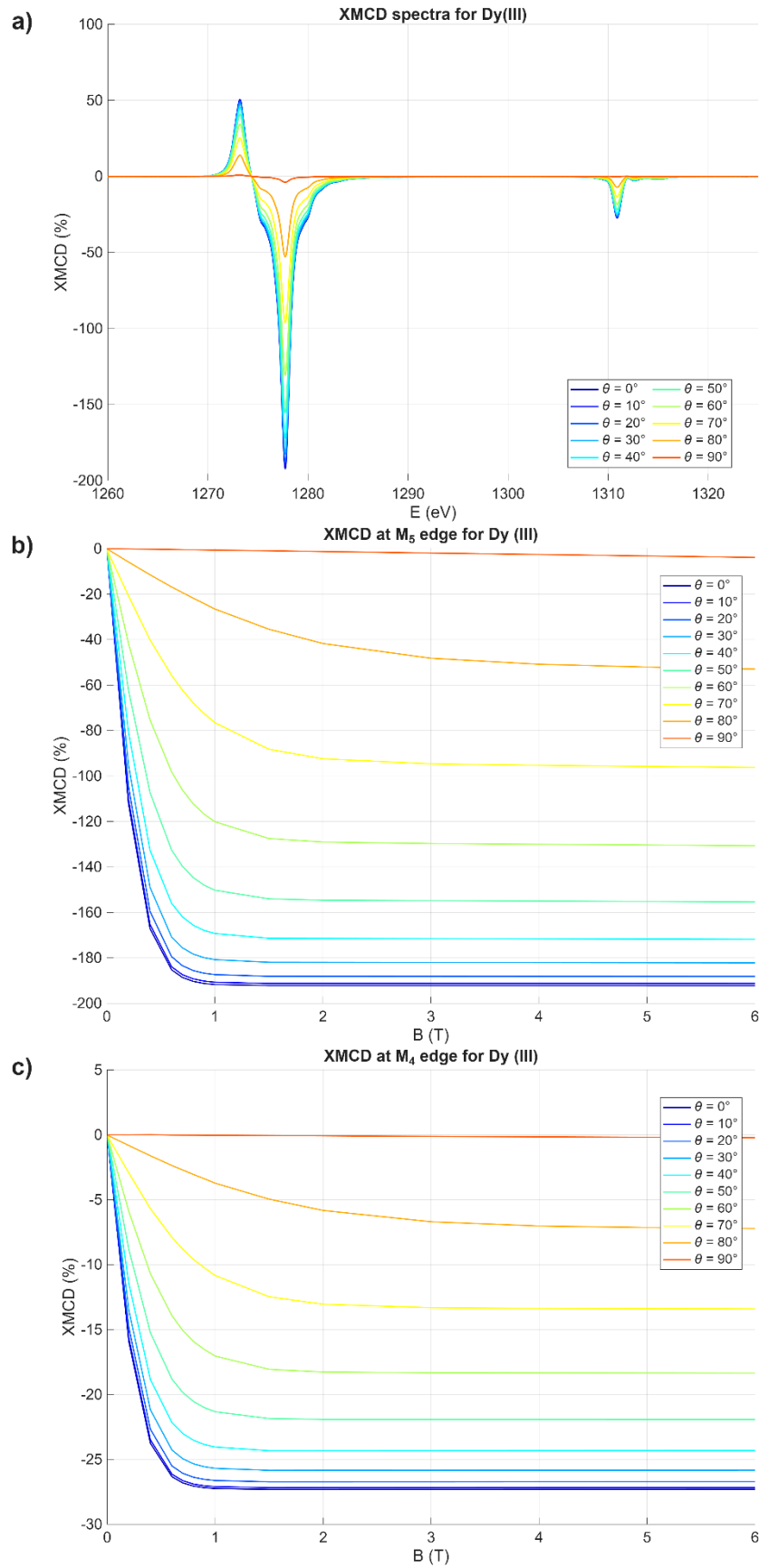


Figure S25 – Angular dependent XMCD spectra at 6 T (a) and angular- and field-dependent XMCD maximum values at M_5 (b) and M_4 (c) edges for Dy(III) centre having a negative B_2^0 value, as discussed in main text.

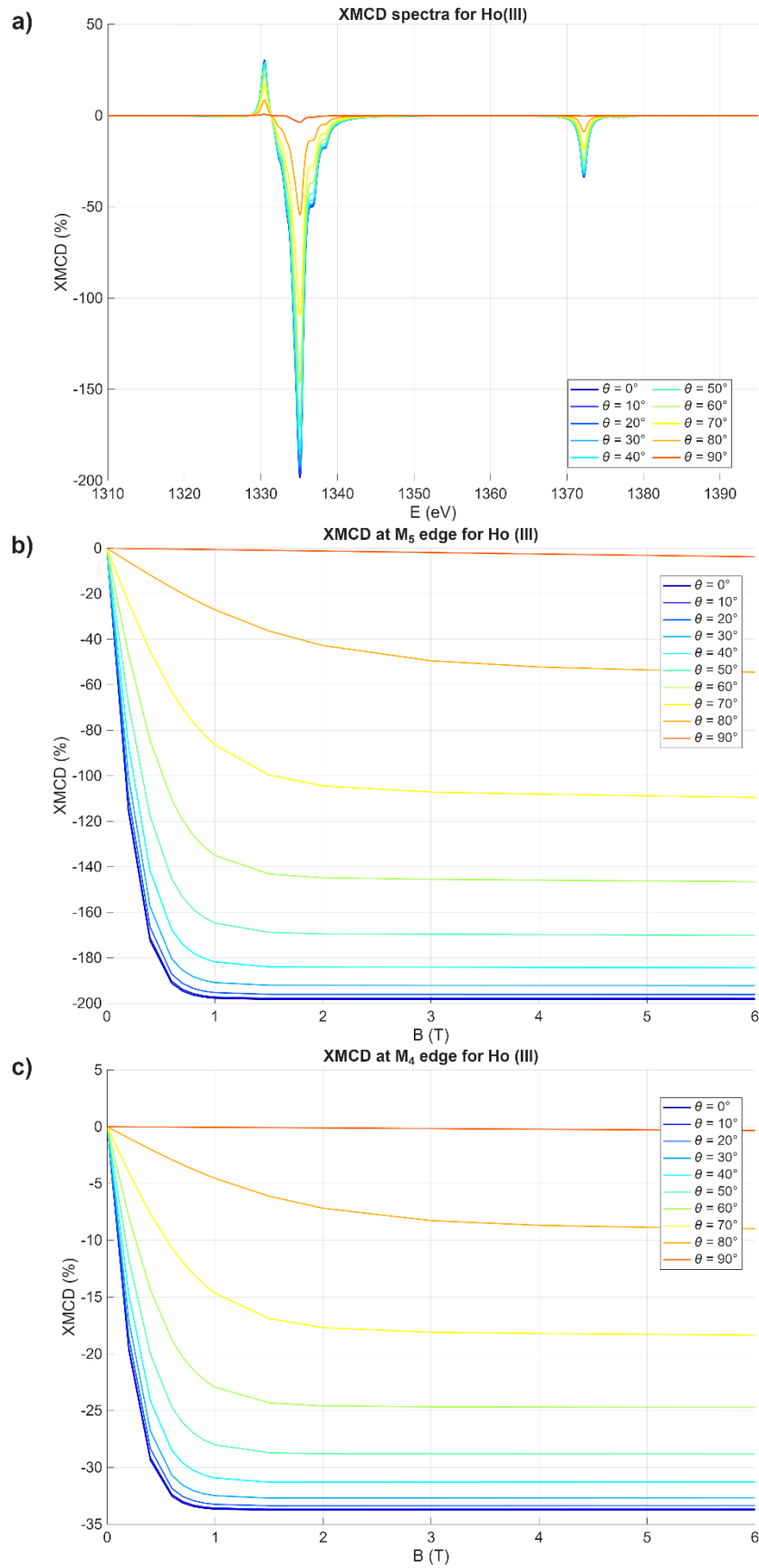


Figure S26 – Angular dependent XMCD spectra at 6 T (a) and angular- and field-dependent XMCD maximum values at M_5 (b) and M_4 (c) edges for Ho(III) centre having a negative B_2^0 value, as discussed in main text.

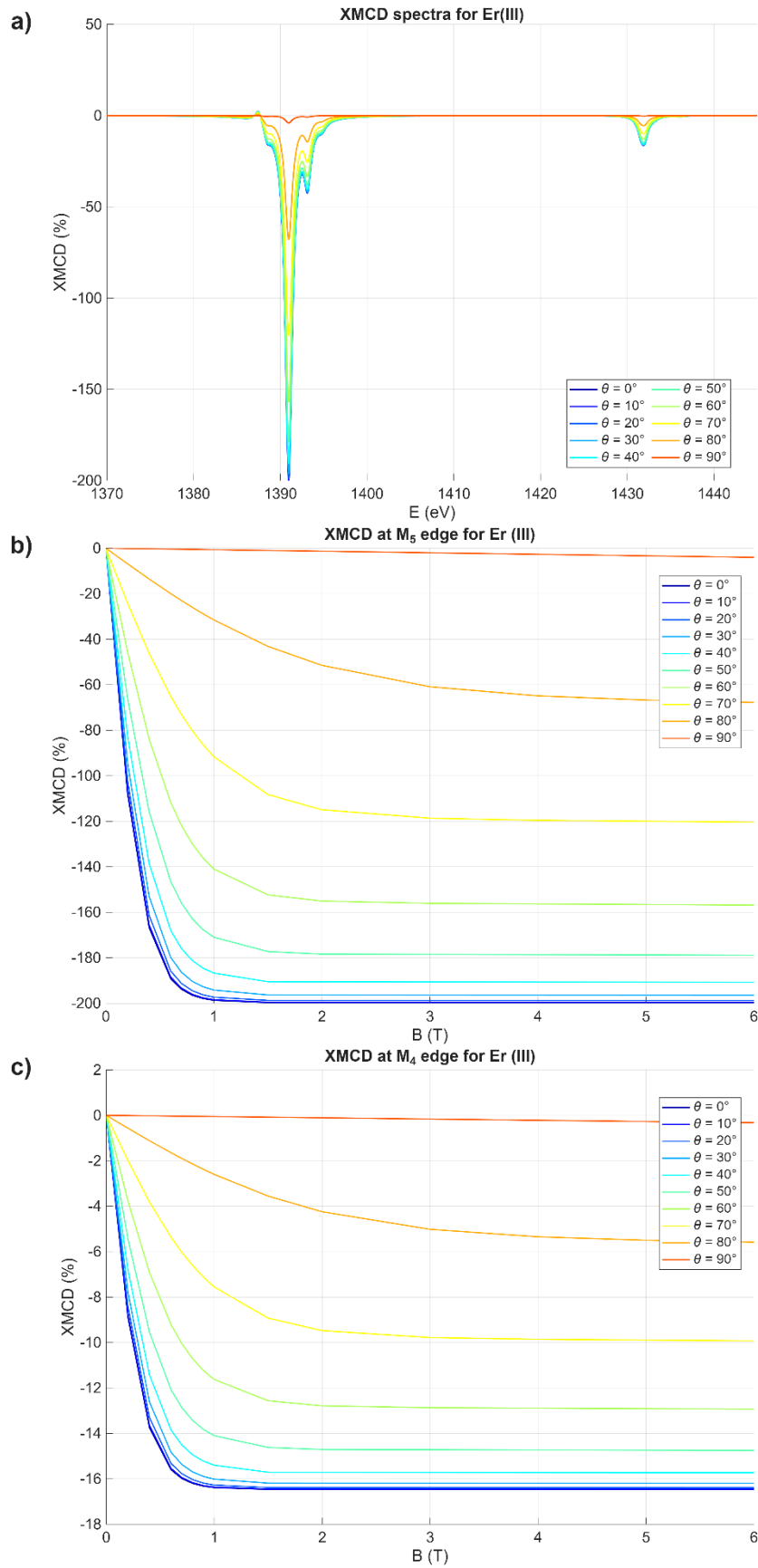


Figure S27 – Angular dependent XMCD spectra at 6 T (a) and angular- and field-dependent XMCD maximum values at M_5 (b) and M_4 (c) edges for Er(III) centre having a negative B_2^0 value, as discussed in main text.

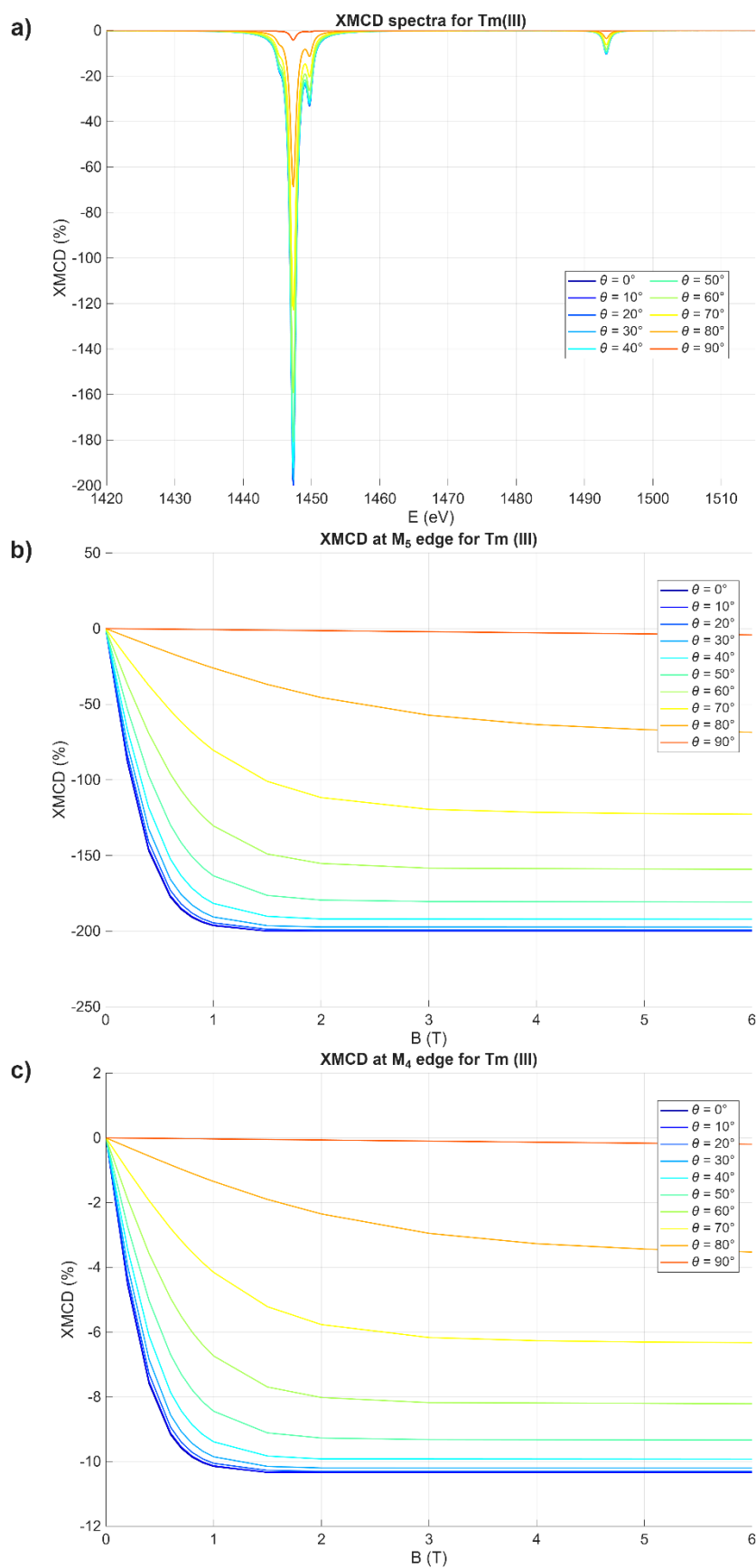


Figure S28 – Angular dependent XMCD spectra at 6 T(a) and angular- and field-dependent XMCD maximum values at M_5 (b) and M_4 (c) edges for Tm(III) centre having a negative B_2^0 value, as discussed in main text.

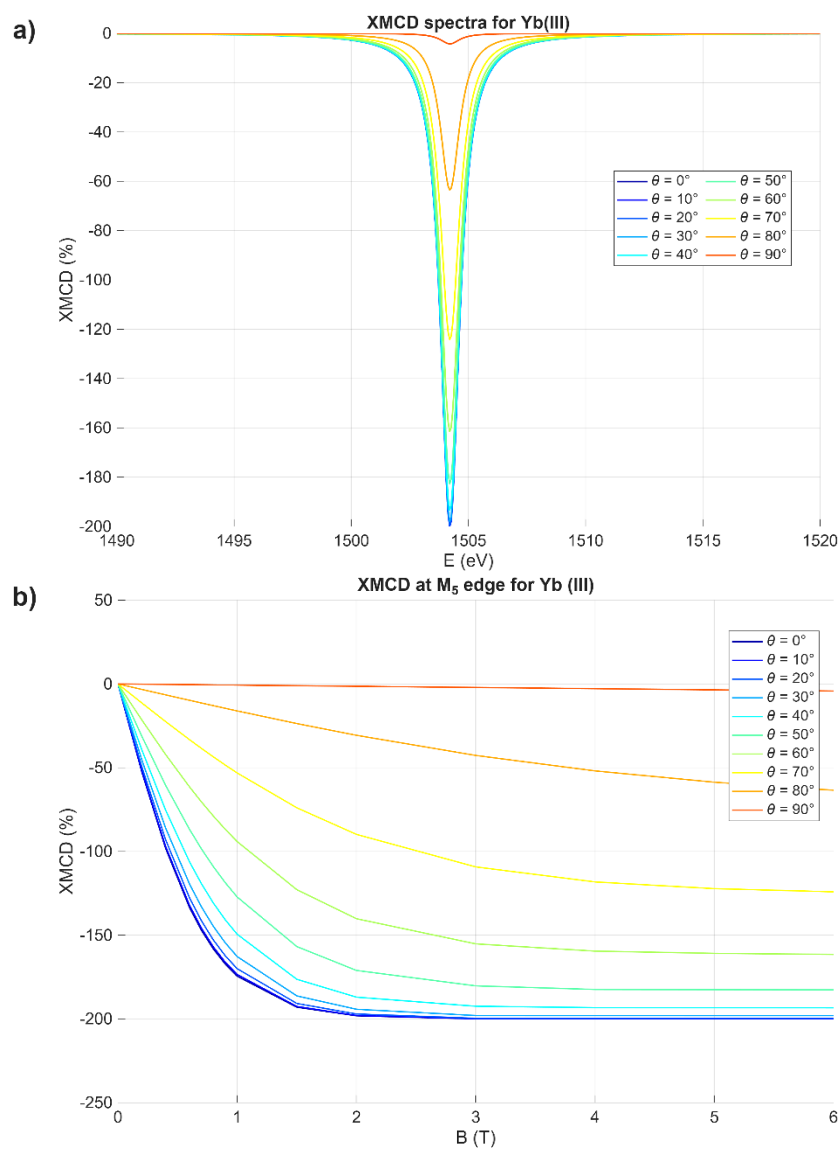


Figure S29 – Angular dependent XMCD spectra at 6 T (a) and angular- and field-dependent XMCD maximum values at M_5 (b) edge for Yb(III) centre having a negative B_2^0 value, as discussed in main text.

Supporting Tables

Table S1 $-B_2^0$ values used for simulating all the magnetic observables of all lanthanide tripositive ions and the associated energy structure of the ground state J multiplet.

	Ce	Pr	Nd	Pm	Sm	Tb	Dy	Ho	Er	Tm	Yb
$B_2^0(cm^{-1})$	-25	-14.3	-12.5	-14.3	-25	-9.1	-7.1	-6.7	-7.1	-9.1	-16.7
$E_1(cm^{-1})$	0	0	0	0	0	0	0	0	0	0	0
$E_2(cm^{-1})$	0	0	0	0	0	0	0	0	0	0	0
$E_3(cm^{-1})$	300	300	300	300	300	300	300	300	300	300	300
$E_4(cm^{-1})$	300	300	300	300	300	300	300	300	300	300	300
$E_5(cm^{-1})$	450	514.3	525	514.3	450	545.4	557.1	560	557.1	545.4	500
$E_6(cm^{-1})$	450	514.3	525	514.3	450	545.4	557.1	560	557.1	545.4	500
$E_7(cm^{-1})$		642.8	675	642.8		736.4	771.4	780	771.4	736.4	600
$E_8(cm^{-1})$		642.8	675	642.8		736.4	771.4	780	771.4	736.4	600
$E_9(cm^{-1})$		685.7	750	685.7		872.7	942.8	960	942.8	872.7	
$E_{10}(cm^{-1})$			750			872.7	942.8	960	942.8	872.7	
$E_{11}(cm^{-1})$						954.5	1071.4	1100	1071.4	954.5	
$E_{12}(cm^{-1})$						954.5	1071.4	1100	1071.4	954.5	
$E_{13}(cm^{-1})$						981.8	1157.1	1200	1157.1	981.8	
$E_{14}(cm^{-1})$							1157.1	1200	1157.1		
$E_{15}(cm^{-1})$							1200	1260	1200		
$E_{16}(cm^{-1})$							1200	1260	1200		
$E_{17}(cm^{-1})$								1280			

Table S2 – Angular- and field-dependent XMCD maximum values at $M_{4,5}$ edges for Ce(III) centre having a negative B_2^0 value, as discussed in main text.

M5 edge													
θ (°)	B = 0.2T	B = 0.4 T	B = 0.6 T	B = 0.7 T	B = 0.8 T	B = 0.9 T	B = 1T	B = 1.5 T	B = 2T	B = 3T	B = 4T	B = 5T	B = 6T
0	8.06	15.81	22.97	26.27	29.37	32.24	34.90	45.00	50.82	55.54	56.76	57.17	57.20
10	7.88	15.47	22.50	25.75	28.80	31.64	34.26	44.32	50.20	55.04	56.32	56.77	56.80
20	7.36	14.46	21.09	24.17	27.08	29.80	32.33	42.24	48.25	53.45	54.93	55.35	55.52
30	6.50	12.80	18.74	21.54	24.19	26.70	29.07	38.58	44.71	50.49	52.33	52.90	53.16
40	5.34	10.56	15.54	17.92	20.20	22.38	24.45	33.17	39.24	45.67	48.08	48.94	49.26
50	4.03	7.99	11.83	13.68	15.48	17.22	18.90	26.31	31.98	38.89	42.06	43.43	44.03
60	2.58	5.13	7.64	8.86	10.07	11.25	12.41	17.74	22.24	28.70	32.45	34.49	35.57
70	1.27	2.54	3.80	4.42	5.04	5.65	6.26	9.17	11.85	16.38	19.75	22.13	23.75
80	0.36	0.71	1.07	1.25	1.42	1.60	1.77	2.65	3.50	5.13	6.64	7.99	9.19
90	0.02	0.05	0.07	0.08	0.10	0.11	0.12	0.18	0.24	0.36	0.48	0.61	0.73
M4 edge													
θ (°)	B = 0.2T	B = 0.4 T	B = 0.6 T	B = 0.7 T	B = 0.8 T	B = 0.9 T	B = 1T	B = 1.5 T	B = 2T	B = 3T	B = 4T	B = 5T	B = 6T
0	-18.52	-36.32	-52.77	-60.36	-67.46	-74.06	-80.15	-103.34	-116.70	-127.50	-130.26	-131.15	-131.17
10	-18.11	-35.54	-51.69	-59.15	-66.15	-72.67	-78.70	-101.80	-115.28	-126.36	-129.26	-130.23	-130.24
20	-16.90	-33.22	-48.44	-55.52	-62.19	-68.45	-74.27	-97.02	-110.80	-122.71	-126.06	-126.97	-127.31
30	-14.92	-29.40	-43.05	-49.47	-55.57	-61.34	-66.76	-88.62	-102.68	-115.91	-120.09	-121.36	-121.91
40	-12.27	-24.26	-35.70	-41.15	-46.39	-51.40	-56.16	-76.18	-90.12	-104.85	-110.34	-112.28	-112.99
50	-9.25	-18.35	-27.16	-31.41	-35.55	-39.55	-43.42	-60.42	-73.42	-89.29	-96.54	-99.65	-100.99
60	-5.92	-11.79	-17.54	-20.35	-23.12	-25.83	-28.49	-40.73	-51.05	-65.87	-74.46	-79.11	-81.57
70	-2.93	-5.84	-8.72	-10.15	-11.57	-12.97	-14.36	-21.04	-27.19	-37.56	-45.30	-50.75	-54.44
80	-0.82	-1.63	-2.44	-2.85	-3.25	-3.66	-4.06	-6.05	-8.00	-11.73	-15.17	-18.27	-21.00
90	-0.05	-0.10	-0.16	-0.18	-0.21	-0.23	-0.26	-0.39	-0.52	-0.78	-1.04	-1.30	-1.56

Table S3 – Angular- and field-dependent XMCD maximum values at $M_{4,5}$ edges for Pr(III) centre having a negative B_2^0 value, as discussed in main text.

M5 edge													
θ (°)	B = 0.2T	B = 0.4 T	B = 0.6 T	B = 0.7 T	B = 0.8 T	B = 0.9 T	B = 1T	B = 1.5 T	B = 2T	B = 3T	B = 4T	B = 5T	B = 6T
0	16.81	32.20	45.16	50.61	55.36	59.46	62.95	73.54	77.54	79.46	79.72	79.72	79.72
10	16.32	31.30	43.98	49.33	54.02	58.07	61.54	72.17	76.27	78.27	78.56	78.56	78.57
20	14.90	28.68	40.51	45.57	50.05	53.97	57.36	68.07	72.44	74.72	75.09	75.11	75.12
30	12.69	24.55	34.96	39.51	43.61	47.25	50.46	61.13	65.90	68.70	69.25	69.27	69.29
40	9.94	19.37	27.88	31.70	35.21	38.41	41.29	51.54	56.75	60.32	61.07	61.28	61.31
50	7.01	13.77	20.05	22.96	25.69	28.25	30.61	39.75	45.17	49.73	50.99	51.35	51.50
60	4.25	8.40	12.37	14.27	16.09	17.83	19.50	26.53	31.49	36.82	38.88	39.65	39.96
70	1.99	3.96	5.89	6.83	7.76	8.67	9.55	13.63	17.03	21.85	24.59	26.05	26.82
80	0.52	1.05	1.57	1.83	2.09	2.34	2.60	3.84	5.03	7.17	8.96	10.40	11.51
90	0.02	0.03	0.05	0.06	0.07	0.07	0.08	0.12	0.17	0.25	0.33	0.41	0.50
M4 edge													
θ (°)	B = 0.2T	B = 0.4 T	B = 0.6 T	B = 0.7 T	B = 0.8 T	B = 0.9 T	B = 1T	B = 1.5 T	B = 2T	B = 3T	B = 4T	B = 5T	B = 6T
0	-24.05	-46.05	-64.60	-72.38	-79.18	-85.04	-90.04	-105.18	-110.90	-113.63	-114.00	-114.00	-113.99
10	-23.35	-44.76	-62.90	-70.55	-77.26	-83.06	-88.02	-103.23	-109.08	-111.94	-112.34	-112.34	-112.34
20	-21.32	-41.02	-57.94	-65.18	-71.59	-77.20	-82.05	-97.36	-103.60	-106.87	-107.39	-107.41	-107.42
30	-18.15	-35.11	-50.01	-56.52	-62.37	-67.59	-72.18	-87.43	-94.25	-98.26	-99.04	-99.07	-99.10
40	-14.22	-27.71	-39.88	-45.35	-50.37	-54.94	-59.07	-73.73	-81.17	-86.29	-87.36	-87.66	-87.71
50	-10.04	-19.70	-28.69	-32.85	-36.76	-40.41	-43.80	-56.87	-64.62	-71.16	-72.96	-73.48	-73.70
60	-6.08	-12.02	-17.70	-20.41	-23.02	-25.52	-27.90	-37.96	-45.05	-52.70	-55.65	-56.76	-57.21
70	-2.85	-5.67	-8.43	-9.78	-11.11	-12.41	-13.68	-19.51	-24.39	-31.29	-35.22	-37.32	-38.43
80	-0.75	-1.50	-2.25	-2.62	-2.99	-3.36	-3.73	-5.52	-7.22	-10.30	-12.87	-14.94	-16.55
90	-0.03	-0.05	-0.08	-0.09	-0.11	-0.12	-0.13	-0.20	-0.27	-0.40	-0.53	-0.67	-0.80

Table S4 – Angular- and field-dependent XMCD maximum values at $M_{4,5}$ edges for Nd(III) centre having a negative B_2^0 value, as discussed in main text.

M5 edge													
θ (°)	B = 0.2T	B = 0.4 T	B = 0.6 T	B = 0.7 T	B = 0.8 T	B = 0.9 T	B = 1T	B = 1.5 T	B = 2T	B = 3T	B = 4T	B = 5T	B = 6T
0	6.79	12.99	18.19	20.36	22.25	23.87	25.25	29.38	30.92	31.65	31.76	31.78	31.80
10	6.61	12.66	17.75	19.90	21.76	23.38	24.75	28.92	30.49	31.26	31.38	31.40	31.42
20	6.08	11.69	16.48	18.52	20.32	21.89	23.25	27.49	29.19	30.07	30.22	30.24	30.26
30	5.25	10.14	14.43	16.29	17.96	19.45	20.75	25.04	26.94	28.03	28.26	28.28	28.31
40	4.19	8.16	11.72	13.32	14.79	16.12	17.31	21.53	23.65	25.08	25.39	25.48	25.51
50	3.02	5.92	8.61	9.85	11.02	12.11	13.11	16.97	19.23	21.12	21.64	21.83	21.87
60	1.87	3.69	5.43	6.26	7.06	7.82	8.54	11.60	13.73	16.01	16.88	17.21	17.35
70	0.89	1.78	2.64	3.06	3.48	3.89	4.28	6.10	7.61	9.74	10.94	11.58	11.92
80	0.24	0.48	0.72	0.84	0.96	1.07	1.19	1.76	2.31	3.29	4.10	4.76	5.27
90	0.01	0.02	0.03	0.04	0.04	0.05	0.05	0.08	0.11	0.16	0.22	0.27	0.33
M4 edge													
θ (°)	B = 0.2T	B = 0.4 T	B = 0.6 T	B = 0.7 T	B = 0.8 T	B = 0.9 T	B = 1T	B = 1.5 T	B = 2T	B = 3T	B = 4T	B = 5T	B = 6T
0	-26.96	-51.56	-72.19	-80.81	-88.31	-94.75	-100.22	-116.62	-122.70	-125.54	-125.91	-125.92	-125.93
10	-26.24	-50.25	-70.48	-78.98	-86.40	-92.79	-98.24	-114.76	-121.00	-123.98	-124.39	-124.40	-124.41
20	-24.14	-46.40	-65.43	-73.53	-80.68	-86.91	-92.28	-109.08	-115.80	-119.25	-119.79	-119.81	-119.83
30	-20.83	-40.27	-57.27	-64.67	-71.31	-77.20	-82.37	-99.38	-106.86	-111.17	-111.99	-112.02	-112.06
40	-16.63	-32.37	-46.53	-52.88	-58.69	-63.96	-68.71	-85.45	-93.81	-99.46	-100.61	-100.92	-100.98
50	-11.97	-23.48	-34.16	-39.09	-43.72	-48.03	-52.02	-67.33	-76.29	-83.71	-85.71	-86.43	-86.52
60	-7.40	-14.63	-21.53	-24.82	-27.98	-31.00	-33.88	-45.98	-54.43	-63.41	-66.81	-68.07	-68.57
70	-3.54	-7.04	-10.46	-12.13	-13.78	-15.38	-16.95	-24.15	-30.13	-38.52	-43.23	-45.72	-47.01
80	-0.95	-1.89	-2.83	-3.29	-3.76	-4.22	-4.68	-6.92	-9.05	-12.89	-16.09	-18.64	-20.61
90	-0.03	-0.06	-0.10	-0.11	-0.13	-0.15	-0.16	-0.24	-0.32	-0.49	-0.65	-0.81	-0.97

Table S5 – Angular- and field-dependent XMCD maximum values at M_{4,5} edges for Pm(III) centre having a negative B_2^0 value, as discussed in main text.

M5 edge													
θ (°)	B = 0.2T	B = 0.4 T	B = 0.6 T	B = 0.7 T	B = 0.8 T	B = 0.9 T	B = 1T	B = 1.5 T	B = 2T	B = 3T	B = 4T	B = 5T	B = 6T
0	6.54	12.77	18.44	21.01	23.40	25.58	27.56	34.80	38.64	41.44	42.06	42.25	42.27
10	6.36	12.43	17.98	20.50	22.83	24.98	26.94	34.13	38.01	40.88	41.54	41.73	41.76
20	5.85	11.45	16.61	18.97	21.18	23.22	25.09	32.13	36.08	39.17	39.94	40.19	40.21
30	5.04	9.90	14.43	16.53	18.51	20.36	22.08	28.78	32.79	36.24	37.20	37.48	37.60
40	4.02	7.92	11.61	13.36	15.02	16.59	18.08	24.13	28.10	31.96	33.24	33.67	33.87
50	2.89	5.72	8.44	9.74	11.00	12.22	13.38	18.39	22.04	26.19	27.91	28.60	28.88
60	1.79	3.55	5.27	6.11	6.93	7.73	8.52	12.07	14.98	18.93	21.05	22.12	22.66
70	0.86	1.71	2.55	2.96	3.37	3.78	4.18	6.10	7.84	10.69	12.71	14.06	14.94
80	0.23	0.47	0.70	0.82	0.93	1.05	1.16	1.73	2.28	3.33	4.29	5.13	5.86
90	-0.02	-0.03	-0.05	-0.06	-0.06	-0.07	-0.08	-0.12	-0.16	-0.24	-0.32	-0.39	-0.47
M4 edge													
θ (°)	B = 0.2T	B = 0.4 T	B = 0.6 T	B = 0.7 T	B = 0.8 T	B = 0.9 T	B = 1T	B = 1.5 T	B = 2T	B = 3T	B = 4T	B = 5T	B = 6T
0	-12.15	-23.74	-34.28	-39.07	-43.49	-47.55	-51.24	-64.68	-71.81	-76.98	-78.12	-78.43	-78.43
10	-11.83	-23.11	-33.42	-38.10	-42.45	-46.44	-50.08	-63.44	-70.63	-75.94	-77.13	-77.47	-77.47
20	-10.87	-21.29	-30.87	-35.26	-39.36	-43.15	-46.64	-59.71	-67.04	-72.75	-74.15	-74.57	-74.59
30	-9.37	-18.40	-26.81	-30.72	-34.40	-37.84	-41.04	-53.47	-60.92	-67.29	-69.05	-69.52	-69.70
40	-7.46	-14.72	-21.58	-24.81	-27.90	-30.82	-33.58	-44.81	-52.17	-59.31	-61.66	-62.40	-62.74
50	-5.36	-10.62	-15.67	-18.09	-20.43	-22.68	-24.84	-34.12	-40.89	-48.57	-51.72	-52.95	-53.43
60	-3.31	-6.58	-9.77	-11.33	-12.85	-14.34	-15.79	-22.37	-27.74	-35.04	-38.94	-40.88	-41.82
70	-1.58	-3.15	-4.70	-5.47	-6.23	-6.98	-7.72	-11.26	-14.46	-19.69	-23.39	-25.85	-27.41
80	-0.42	-0.84	-1.26	-1.47	-1.68	-1.89	-2.09	-3.12	-4.11	-6.00	-7.70	-9.20	-10.49
90	-0.01	-0.03	-0.04	-0.05	-0.05	-0.06	-0.07	-0.10	-0.13	-0.20	-0.27	-0.33	-0.40

Table S6 – Angular- and field-dependent XMCD maximum values at $M_{4,5}$ edges for Sm(III) centre having a negative B_2^0 value, as discussed in main text.

M5 edge													
θ (°)	B = 0.2T	B = 0.4 T	B = 0.6 T	B = 0.7 T	B = 0.8 T	B = 0.9 T	B = 1T	B = 1.5 T	B = 2T	B = 3T	B = 4T	B = 5T	B = 6T
0	2.77	5.50	8.35	9.61	10.96	12.32	13.64	20.23	26.50	38.08	47.51	55.28	61.39
10	2.68	5.36	7.97	9.35	10.67	11.99	13.29	19.43	25.82	36.98	46.43	54.11	60.13
20	2.47	4.93	7.39	8.61	9.83	11.04	12.24	18.15	23.83	34.28	43.22	50.62	56.53
30	2.13	4.26	6.37	7.50	8.45	9.54	10.58	15.73	20.68	29.90	38.00	44.86	50.50
40	1.66	3.40	5.09	6.00	6.78	7.62	8.46	12.59	16.64	24.66	31.06	37.06	42.18
50	1.23	2.45	3.67	4.25	4.85	5.50	6.12	9.09	12.05	17.71	22.97	27.74	31.98
60	0.76	1.52	2.27	2.65	3.03	3.40	3.78	5.65	7.55	11.11	14.56	17.83	20.84
70	0.36	0.73	1.10	1.27	1.46	1.64	1.82	2.72	3.62	5.41	7.15	8.84	10.48
80	0.10	0.21	0.30	0.35	0.40	0.45	0.50	0.68	1.01	1.51	2.00	2.50	2.99
90	-0.02	-0.03	-0.05	-0.05	-0.06	-0.06	-0.07	-0.11	-0.16	-0.20	-0.30	-0.35	-0.45
M5 edge													
θ (°)	B = 0.2T	B = 0.4 T	B = 0.6 T	B = 0.7 T	B = 0.8 T	B = 0.9 T	B = 1T	B = 1.5 T	B = 2T	B = 3T	B = 4T	B = 5T	B = 6T
0	-1.69	-3.36	-5.09	-5.86	-6.69	-7.51	-8.32	-12.34	-16.17	-23.23	-28.98	-33.72	-37.45
10	-1.64	-3.27	-4.86	-5.70	-6.51	-7.31	-8.11	-11.85	-15.75	-22.55	-28.32	-33.00	-36.67
20	-1.51	-3.01	-4.50	-5.25	-5.99	-6.73	-7.46	-11.07	-14.53	-20.90	-26.35	-30.86	-34.46
30	-1.30	-2.60	-3.88	-4.57	-5.15	-5.81	-6.45	-9.59	-12.60	-18.22	-23.16	-27.34	-30.76
40	-1.03	-2.07	-3.10	-3.64	-4.13	-4.64	-5.15	-7.66	-10.13	-15.02	-18.91	-22.56	-25.67
50	-0.74	-1.49	-2.23	-2.59	-2.95	-3.34	-3.72	-5.53	-7.33	-10.76	-13.95	-16.85	-19.42
60	-0.46	-0.92	-1.37	-1.60	-1.83	-2.06	-2.29	-3.42	-4.56	-6.72	-8.81	-10.78	-12.60
70	-0.22	-0.43	-0.64	-0.76	-0.88	-0.98	-1.09	-1.63	-2.16	-3.23	-4.27	-5.28	-6.26
80	-0.05	-0.12	-0.17	-0.20	-0.23	-0.25	-0.28	-0.37	-0.56	-0.84	-1.12	-1.40	-1.67
90	0.01	0.01	0.01	-0.01	-0.01	-0.01	0.02	0.02	0.04	-0.05	0.07	-0.08	0.10

Table S7 – Angular- and field-dependent XMCD maximum values at $M_{4,5}$ edges for Tb(III) centre having a negative B_2^0 value, as discussed in main text.

M5 edge													
θ (°)	B = 0.2T	B = 0.4 T	B = 0.6 T	B = 0.7 T	B = 0.8 T	B = 0.9 T	B = 1T	B = 1.5 T	B = 2T	B = 3T	B = 4T	B = 5T	B = 6T
0	-98.90	-153.23	-173.98	-178.34	-180.76	-182.10	-182.84	-183.74	-183.74	-183.74	-183.74	-183.74	-183.74
10	-97.28	-151.51	-172.64	-177.15	-179.68	-181.10	-181.89	-182.87	-182.87	-182.88	-182.88	-182.89	-182.89
20	-91.97	-145.95	-168.22	-173.20	-176.10	-177.76	-178.73	-180.00	-180.02	-180.04	-180.06	-180.08	-180.10
30	-83.26	-135.65	-159.58	-165.41	-168.96	-171.13	-172.41	-174.34	-174.37	-174.42	-174.48	-174.53	-174.59
40	-70.83	-119.38	-144.91	-151.82	-156.37	-159.32	-161.20	-164.19	-164.58	-164.70	-164.81	-164.93	-165.04
50	-54.61	-96.20	-122.03	-129.76	-135.57	-139.58	-142.39	-147.72	-148.73	-148.95	-149.17	-149.39	-149.61
60	-30.98	-57.48	-76.71	-83.69	-89.29	-93.62	-97.00	-104.99	-107.06	-108.09	-108.60	-109.11	-109.62
70	-13.80	-26.54	-37.42	-42.13	-46.20	-49.86	-52.86	-62.61	-66.62	-69.03	-69.81	-70.31	-70.80
80	-3.42	-6.96	-10.25	-11.84	-13.33	-14.79	-16.21	-22.23	-26.63	-31.56	-33.81	-34.93	-35.64
90	-0.09	-0.19	-0.28	-0.33	-0.38	-0.42	-0.47	-0.71	-0.94	-1.41	-1.88	-2.35	-2.82
M4 edge													
θ (°)	B = 0.2T	B = 0.4 T	B = 0.6 T	B = 0.7 T	B = 0.8 T	B = 0.9 T	B = 1T	B = 1.5 T	B = 2T	B = 3T	B = 4T	B = 5T	B = 6T
0	8.72	13.50	15.33	15.72	15.93	16.05	16.11	16.19	16.19	16.19	16.19	16.19	16.19
10	8.57	13.35	15.22	15.61	15.84	15.96	16.03	16.12	16.12	16.12	16.12	16.12	16.13
20	8.11	12.87	14.83	15.27	15.52	15.67	15.76	15.87	15.88	15.88	15.89	15.90	15.91
30	7.34	11.96	14.08	14.59	14.90	15.09	15.21	15.38	15.39	15.41	15.43	15.44	15.46
40	6.25	10.53	12.79	13.40	13.80	14.06	14.23	14.50	14.55	14.58	14.61	14.65	14.68
50	4.82	8.49	10.78	11.47	11.98	12.34	12.58	13.07	13.18	13.23	13.28	13.34	13.39
60	2.74	5.08	6.78	7.41	7.90	8.29	8.59	9.32	9.52	9.65	9.73	9.82	9.90
70	1.23	2.35	3.33	3.74	4.10	4.43	4.70	5.59	5.96	6.22	6.33	6.42	6.51
80	0.31	0.63	0.93	1.08	1.21	1.35	1.48	2.03	2.46	2.92	3.17	3.31	3.42
90	0.02	0.04	0.06	0.06	0.08	0.08	0.09	0.14	0.18	0.27	0.36	0.45	0.54

Table S8 – Angular- and field-dependent XMCD maximum values at $M_{4,5}$ edges for Dy(III) centre having a negative B_2^0 value, as discussed in main text.

M5 edge													
θ (°)	B = 0.2T	B = 0.4 T	B = 0.6 T	B = 0.7 T	B = 0.8 T	B = 0.9 T	B = 1T	B = 1.5 T	B = 2T	B = 3T	B = 4T	B = 5T	B = 6T
0	-111.89	-167.14	-185.27	-188.61	-190.34	-191.25	-191.71	-192.20	-192.20	-192.20	-192.20	-192.20	-192.20
10	-109.96	-165.28	-183.92	-187.41	-189.24	-190.20	-190.70	-191.24	-191.24	-191.25	-191.25	-191.26	-191.26
20	-104.30	-159.54	-179.48	-183.44	-185.59	-186.75	-187.37	-188.10	-188.10	-188.12	-188.14	-188.16	-188.18
30	-94.91	-148.99	-170.84	-175.58	-178.34	-179.91	-180.79	-181.94	-181.96	-182.01	-182.06	-182.11	-182.16
40	-80.38	-132.61	-156.02	-161.95	-165.63	-167.92	-169.26	-171.38	-171.43	-171.54	-171.64	-171.75	-171.85
50	-62.09	-107.25	-132.59	-139.73	-144.68	-147.99	-150.25	-154.03	-154.63	-154.83	-155.02	-155.22	-155.41
60	-41.52	-75.34	-98.20	-106.15	-112.26	-116.75	-120.13	-127.49	-129.05	-129.71	-130.04	-130.37	-130.70
70	-20.69	-40.12	-55.78	-62.24	-67.84	-72.47	-76.56	-88.22	-92.44	-94.65	-95.32	-95.79	-96.26
80	-5.86	-11.49	-16.86	-19.32	-21.80	-24.16	-26.56	-35.44	-41.73	-48.22	-50.85	-52.08	-52.97
90	-0.13	-0.26	-0.39	-0.45	-0.52	-0.58	-0.65	-0.97	-1.29	-1.94	-2.59	-3.23	-3.88
M4 edge													
θ (°)	B = 0.2T	B = 0.4 T	B = 0.6 T	B = 0.7 T	B = 0.8 T	B = 0.9 T	B = 1T	B = 1.5 T	B = 2T	B = 3T	B = 4T	B = 5T	B = 6T
0	-15.91	-23.76	-26.34	-26.81	-27.06	-27.19	-27.25	-27.32	-27.32	-27.32	-27.32	-27.32	-27.32
10	-15.63	-23.50	-26.15	-26.64	-26.90	-27.04	-27.11	-27.18	-27.18	-27.18	-27.18	-27.18	-27.18
20	-14.83	-22.68	-25.51	-26.07	-26.38	-26.54	-26.63	-26.73	-26.73	-26.73	-26.72	-26.72	-26.72
30	-13.49	-21.18	-24.28	-24.95	-25.34	-25.57	-25.69	-25.85	-25.84	-25.84	-25.84	-25.83	-25.83
40	-11.42	-18.85	-22.17	-23.01	-23.53	-23.86	-24.05	-24.34	-24.34	-24.33	-24.33	-24.33	-24.32
50	-8.82	-15.24	-18.82	-19.85	-20.55	-21.01	-21.33	-21.86	-21.93	-21.93	-21.93	-21.93	-21.93
60	-5.90	-10.69	-13.94	-15.06	-15.93	-16.54	-17.04	-18.06	-18.27	-18.33	-18.34	-18.35	-18.36
70	-2.93	-5.69	-7.90	-8.82	-9.61	-10.24	-10.84	-12.47	-13.05	-13.32	-13.37	-13.39	-13.41
80	-0.82	-1.61	-2.37	-2.71	-3.05	-3.39	-3.73	-4.96	-5.82	-6.70	-7.02	-7.14	-7.22
90	0.00	0.01	-0.02	-0.03	-0.03	-0.04	-0.04	-0.06	-0.07	-0.12	-0.16	-0.19	-0.22

Table S9 – Angular- and field-dependent XMCD maximum values at $M_{4,5}$ edges for Ho(III) centre having a negative B_2^0 value, as discussed in main text.

M5 edge													
θ (°)	B = 0.2T	B = 0.4 T	B = 0.6 T	B = 0.7 T	B = 0.8 T	B = 0.9 T	B = 1T	B = 1.5 T	B = 2T	B = 3T	B = 4T	B = 5T	B = 6T
0	-115.56	-172.52	-191.15	-194.59	-196.38	-197.31	-197.78	-198.29	-198.29	-198.29	-198.29	-198.29	-198.29
10	-113.94	-171.11	-190.25	-193.85	-195.74	-196.73	-197.24	-197.80	-197.80	-197.80	-197.81	-197.81	-197.81
20	-108.92	-166.45	-187.10	-191.21	-193.44	-194.64	-195.29	-196.04	-196.05	-196.06	-196.07	-196.08	-196.09
30	-100.01	-157.35	-180.39	-185.42	-188.30	-189.94	-190.86	-192.07	-192.09	-192.12	-192.15	-192.18	-192.22
40	-86.54	-141.71	-167.53	-173.92	-177.86	-180.28	-181.75	-184.00	-184.05	-184.14	-184.23	-184.32	-184.41
50	-68.38	-117.57	-145.20	-153.19	-158.62	-162.26	-164.68	-168.81	-169.45	-169.63	-169.81	-169.99	-170.17
60	-46.57	-84.41	-110.32	-119.26	-126.06	-131.16	-134.94	-143.12	-144.85	-145.54	-145.87	-146.19	-146.51
70	-23.72	-45.19	-62.93	-70.25	-76.55	-81.91	-86.41	-99.65	-104.49	-107.16	-108.09	-108.79	-109.49
80	-5.95	-11.75	-17.26	-19.88	-22.38	-24.76	-27.02	-36.38	-42.76	-49.47	-52.19	-53.51	-54.47
90	-0.13	-0.25	-0.38	-0.44	-0.51	-0.57	-0.63	-0.95	-1.27	-1.90	-2.53	-3.16	-3.80
M4 edge													
θ (°)	B = 0.2T	B = 0.4 T	B = 0.6 T	B = 0.7 T	B = 0.8 T	B = 0.9 T	B = 1T	B = 1.5 T	B = 2T	B = 3T	B = 4T	B = 5T	B = 6T
0	-19.67	-29.37	-32.54	-33.13	-33.43	-33.59	-33.67	-33.76	-33.76	-33.76	-33.76	-33.75	-33.75
10	-19.40	-29.13	-32.39	-33.00	-33.32	-33.49	-33.58	-33.67	-33.67	-33.67	-33.67	-33.67	-33.67
20	-18.54	-28.34	-31.85	-32.55	-32.93	-33.13	-33.24	-33.37	-33.37	-33.36	-33.36	-33.36	-33.35
30	-17.02	-26.78	-30.71	-31.56	-32.05	-32.33	-32.48	-32.68	-32.68	-32.68	-32.67	-32.67	-32.66
40	-14.73	-24.12	-28.51	-29.60	-30.27	-30.68	-30.92	-31.30	-31.30	-31.29	-31.29	-31.29	-31.29
50	-11.64	-20.01	-24.70	-26.06	-26.98	-27.60	-28.01	-28.70	-28.79	-28.80	-28.80	-28.80	-28.80
60	-7.92	-14.36	-18.76	-20.28	-21.43	-22.30	-22.94	-24.31	-24.58	-24.66	-24.68	-24.69	-24.71
70	-4.03	-7.67	-10.69	-11.93	-12.99	-13.90	-14.66	-16.89	-17.69	-18.10	-18.21	-18.28	-18.35
80	-1.00	-1.98	-2.91	-3.35	-3.77	-4.17	-4.55	-6.12	-7.18	-8.27	-8.68	-8.86	-8.97
90	-0.01	-0.02	-0.03	-0.04	-0.05	-0.05	-0.06	-0.08	-0.11	-0.17	-0.23	-0.28	-0.34

Table S10 – Angular- and field-dependent XMCD maximum values at $M_{4,5}$ edges for Er(III) centre having a negative B_2^0 value, as discussed in main text.

M5 edge													
θ (°)	B = 0.2T	B = 0.4 T	B = 0.6 T	B = 0.7 T	B = 0.8 T	B = 0.9 T	B = 1T	B = 1.5 T	B = 2T	B = 3T	B = 4T	B = 5T	B = 6T
0	-107.52	-166.70	-189.17	-193.85	-196.46	-197.90	-198.70	-199.66	-199.66	-199.66	-199.66	-199.66	-199.66
10	-106.13	-165.44	-188.44	-193.31	-196.05	-197.58	-198.44	-199.49	-199.50	-199.50	-199.50	-199.50	-199.50
20	-101.79	-161.25	-185.79	-191.26	-194.44	-196.27	-197.31	-198.70	-198.70	-198.70	-198.71	-198.71	-198.72
30	-93.99	-152.92	-179.83	-186.35	-190.33	-192.74	-194.18	-196.31	-196.32	-196.34	-196.35	-196.37	-196.39
40	-82.12	-138.49	-167.95	-175.95	-181.19	-184.57	-186.73	-190.50	-190.52	-190.58	-190.63	-190.68	-190.74
50	-65.74	-115.73	-146.41	-155.99	-162.82	-167.63	-170.98	-177.24	-178.37	-178.50	-178.63	-178.75	-178.88
60	-45.47	-83.78	-111.67	-121.85	-129.90	-136.17	-140.99	-152.33	-155.06	-156.06	-156.32	-156.57	-156.82
70	-24.04	-46.17	-65.07	-73.10	-80.18	-86.34	-91.65	-108.25	-114.94	-118.65	-119.56	-119.99	-120.41
80	-6.84	-13.53	-19.95	-23.02	-25.98	-28.82	-31.54	-43.14	-51.49	-60.88	-64.90	-66.74	-67.78
90	-0.13	-0.27	-0.40	-0.47	-0.54	-0.61	-0.67	-1.01	-1.34	-2.02	-2.69	-3.36	-4.03
M4 edge													
θ (°)	B = 0.2T	B = 0.4 T	B = 0.6 T	B = 0.7 T	B = 0.8 T	B = 0.9 T	B = 1T	B = 1.5 T	B = 2T	B = 3T	B = 4T	B = 5T	B = 6T
0	-8.87	-13.75	-15.60	-15.99	-16.20	-16.32	-16.39	-16.47	-16.47	-16.47	-16.47	-16.47	-16.47
10	-8.75	-13.64	-15.54	-15.94	-16.17	-16.30	-16.37	-16.45	-16.45	-16.45	-16.45	-16.45	-16.45
20	-8.39	-13.30	-15.32	-15.77	-16.04	-16.19	-16.27	-16.39	-16.39	-16.39	-16.39	-16.39	-16.39
30	-7.75	-12.61	-14.83	-15.37	-15.70	-15.90	-16.01	-16.19	-16.19	-16.19	-16.19	-16.20	-16.20
40	-6.77	-11.42	-13.85	-14.51	-14.94	-15.22	-15.40	-15.71	-15.71	-15.72	-15.72	-15.73	-15.73
50	-5.42	-9.54	-12.07	-12.86	-13.43	-13.82	-14.10	-14.62	-14.71	-14.72	-14.73	-14.74	-14.75
60	-3.75	-6.91	-9.21	-10.05	-10.71	-11.23	-11.63	-12.56	-12.79	-12.87	-12.89	-12.91	-12.93
70	-1.98	-3.81	-5.37	-6.03	-6.61	-7.12	-7.56	-8.93	-9.48	-9.78	-9.86	-9.89	-9.92
80	-0.56	-1.12	-1.64	-1.90	-2.14	-2.38	-2.60	-3.56	-4.24	-5.02	-5.35	-5.50	-5.58
90	-0.01	-0.02	-0.03	-0.04	-0.04	-0.05	-0.05	-0.08	-0.11	-0.16	-0.22	-0.27	-0.33

Table S11 – Angular- and field-dependent XMCD maximum values at $M_{4,5}$ edges for Tm(III) centre having a negative B_2^0 value, as discussed in main text.

M5 edge													
θ (°)	B = 0.2T	B = 0.4 T	B = 0.6 T	B = 0.7 T	B = 0.8 T	B = 0.9 T	B = 1T	B = 1.5 T	B = 2T	B = 3T	B = 4T	B = 5T	B = 6T
0	-87.58	-146.97	-177.45	-185.60	-190.88	-194.25	-196.39	-200.00	-200.00	-200.00	-200.00	-200.00	-200.00
10	-86.38	-145.57	-176.44	-184.80	-190.26	-193.78	-196.02	-199.91	-199.91	-199.91	-199.91	-199.91	-199.91
20	-82.66	-141.06	-172.95	-181.95	-187.97	-191.94	-194.54	-198.78	-199.32	-199.32	-199.32	-199.33	-199.33
30	-76.08	-132.46	-165.64	-175.63	-182.59	-187.37	-190.62	-196.39	-197.28	-197.29	-197.31	-197.33	-197.34
40	-66.21	-118.33	-152.17	-163.28	-171.47	-177.41	-181.67	-190.19	-191.95	-192.00	-192.05	-192.10	-192.15
50	-52.81	-97.26	-129.58	-141.35	-150.64	-157.87	-163.43	-176.40	-179.45	-180.43	-180.56	-180.68	-180.80
60	-36.42	-69.17	-95.90	-106.79	-116.08	-123.91	-130.42	-148.98	-155.28	-158.38	-158.64	-158.89	-159.14
70	-19.23	-37.51	-54.08	-61.55	-68.44	-74.74	-80.44	-100.98	-111.70	-119.49	-121.45	-122.28	-122.71
80	-5.49	-10.91	-16.19	-18.76	-21.27	-23.73	-26.11	-36.88	-45.58	-57.25	-63.50	-66.77	-68.60
90	-0.14	-0.28	-0.42	-0.49	-0.56	-0.63	-0.70	-1.05	-1.40	-2.11	-2.81	-3.51	-4.21
M4 edge													
θ (°)	B = 0.2T	B = 0.4 T	B = 0.6 T	B = 0.7 T	B = 0.8 T	B = 0.9 T	B = 1T	B = 1.5 T	B = 2T	B = 3T	B = 4T	B = 5T	B = 6T
0	-4.53	-7.60	-9.17	-9.60	-9.87	-10.04	-10.15	-10.34	-10.34	-10.34	-10.34	-10.34	-10.34
10	-4.47	-7.53	-9.12	-9.55	-9.84	-10.02	-10.13	-10.34	-10.34	-10.34	-10.34	-10.34	-10.34
20	-4.27	-7.29	-8.94	-9.41	-9.72	-9.92	-10.06	-10.28	-10.30	-10.30	-10.30	-10.30	-10.30
30	-3.93	-6.85	-8.56	-9.08	-9.44	-9.69	-9.85	-10.15	-10.20	-10.20	-10.20	-10.20	-10.20
40	-3.42	-6.12	-7.87	-8.44	-8.86	-9.17	-9.39	-9.83	-9.92	-9.92	-9.93	-9.93	-9.93
50	-2.73	-5.03	-6.70	-7.31	-7.79	-8.16	-8.45	-9.12	-9.27	-9.32	-9.33	-9.33	-9.34
60	-1.88	-3.57	-4.96	-5.52	-6.00	-6.40	-6.74	-7.70	-8.02	-8.18	-8.19	-8.20	-8.22
70	-0.99	-1.94	-2.79	-3.18	-3.54	-3.86	-4.16	-5.22	-5.77	-6.17	-6.27	-6.31	-6.33
80	-0.28	-0.56	-0.84	-0.97	-1.10	-1.22	-1.35	-1.90	-2.35	-2.95	-3.27	-3.44	-3.53
90	-0.01	-0.01	-0.02	-0.02	-0.03	-0.03	-0.03	-0.05	-0.07	-0.10	-0.13	-0.16	-0.20

Table S12 – Angular- and field-dependent XMCD maximum values at $M_{4,5}$ edges for Yb(III) centre having a negative B_2^0 value, as discussed in main text.

M5 edge													
θ (°)	B = 0.2T	B = 0.4 T	B = 0.6 T	B = 0.7 T	B = 0.8 T	B = 0.9 T	B = 1T	B = 1.5 T	B = 2T	B = 3T	B = 4T	B = 5T	B = 6T
0	-52.48	-98.20	-133.48	-147.08	-158.25	-167.28	-174.50	-193.02	-198.15	-200.00	-200.00	-200.00	-200.00
10	-51.71	-96.95	-132.10	-145.74	-157.00	-166.14	-173.49	-192.56	-197.97	-199.98	-199.98	-199.98	-199.98
20	-49.36	-93.04	-127.68	-141.39	-152.87	-162.32	-170.03	-190.78	-197.08	-199.62	-199.62	-199.63	-199.63
30	-45.27	-86.03	-119.43	-133.07	-144.73	-154.58	-162.79	-186.27	-194.25	-197.99	-198.01	-198.02	-198.03
40	-39.23	-75.35	-106.17	-119.26	-130.80	-140.84	-149.48	-176.36	-187.02	-192.44	-193.29	-193.34	-193.38
50	-31.17	-60.57	-86.80	-98.46	-109.08	-118.66	-127.22	-156.81	-171.07	-180.28	-182.42	-182.54	-182.66
60	-21.45	-42.15	-61.44	-70.41	-78.86	-86.78	-94.14	-122.85	-140.19	-155.20	-159.54	-160.87	-161.50
70	-11.34	-22.48	-33.27	-38.47	-43.53	-48.43	-53.16	-73.95	-89.84	-109.25	-118.23	-122.24	-124.12
80	-3.28	-6.54	-9.78	-11.38	-12.97	-14.55	-16.11	-23.67	-30.67	-42.69	-51.93	-58.68	-63.48
90	-0.14	-0.28	-0.42	-0.50	-0.57	-0.64	-0.71	-1.06	-1.42	-2.12	-2.83	-3.54	-4.25

Supporting Notes

Note S1. Normalization procedure of XMCD spectra.

XMCD spectra are experimentally obtained by recording the absorption spectra with right- and left-handed circularly polarized X-rays, denoted as σ_r and σ_l , respectively, and calculating their difference.

$$\sigma_{XMCD} = \sigma_r - \sigma_l$$

The absolute magnitude of the experimental XMCD signal is typically reported in arbitrary units, as it strongly depends on instrumental factors such as beamline characteristics and detection efficiency. To enable comparison between spectra collected at different beamlines, or between experimental and simulated data, the XMCD signal is commonly normalized.

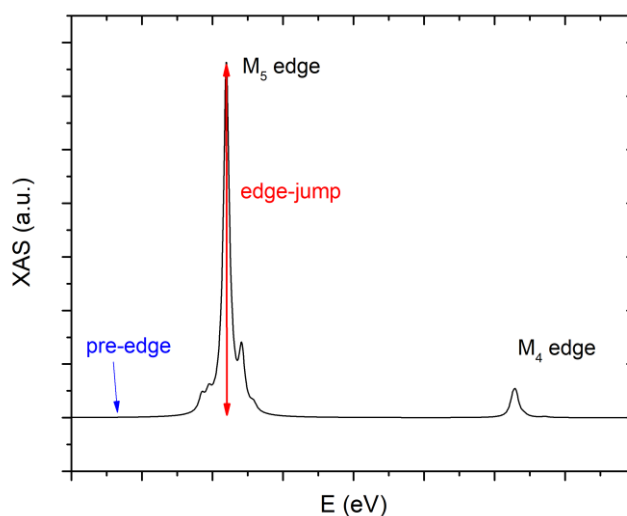
The isotropic absorption spectrum is defined as the average of the two polarization dependent spectra, as follows.

$$\sigma_{isotropic} = \frac{\sigma_r + \sigma_l}{2}$$

The normalized XMCD intensity (expressed as a percentage) is obtained by dividing the XMCD signal by the isotropic edge-jump at the selected absorption edge (either M_4 or M_5) and multiplying by 100.

$$\sigma_{XMCD}(\%) = \frac{\sigma_{XMCD}}{ej_{iso}} * 100$$

The edge-jump (ej_{iso}) is defined as the difference between the maximum absorption intensity at the selected edge and the pre-edge baseline value of the isotropic spectrum, as schematically illustrated below.



In this work, all XMCD spectra were normalized with respect to the isotropic edge-jump at the M_5 absorption edge.